IMPROVED DROUGHT EARLY WARNING AND FORECASTING TO STRENGTHEN PREPAREDNESS AND ADAPTATION TO DROUGHTS IN AFRICA

DEWFORA

A 7th Framework Programme Collaborative Research Project

Impacts of climate change on drought hazards over Africa

WP3-Task3.2-D3.6

December 2013

Coordinator:	Deltares, The Netherlands
Project website:	www.dewfora.net
FP7 Call	ENV-2010-1.3.3.1
Contract no.	265454

Page intentionally left blank

DOCUMENT INFORMATION

Title	Impacts of climate change on drought hazards over Africa
Lead Author	Francois Engelbrecht, Hessel Winsemius, Paulo Barbosa and Gustavo Naumann
Contributors	Emma Archer Van Garderen Mary-Jane Bopape Emanuel Dutra Willem Landman Mogesh Naidoo Florian Pappenberger Jacobus Van der Merwe Micha Werner Fredrik Wetterhall
Distribution	PP
Reference	WP3-Task3.2-D3.6

DOCUMENT HISTORY

Date	Revision	Prepared by	Organisation	Approved by	Notes
20/12/2013		Francois Engelbrecht	CSIR		

ACKNOWLEDGEMENT

The research leading to these results has received funding from the European Union's Seventh Framework Programme (FP7/2007-2013) under grant agreement N°265454

Page intentionally left blank

SUMMARY

In this component of the DEWFORA research the impact of enhanced anthropogenic forcing on the attributes of drought over the African continent are explored. The analysis presented is largely based on high-resolution projections of climate change over Africa, performed as a part of DEWFORA, and were obtained using a variable-resolution global model to downscale the projections of a number of CGCMs over Africa. The regional model simulations were first bias-corrected using observed monthly climatologies from CRU, before being used to study a number of drought metrics and their projected changes. The research conclusions also rely on the analysis of CGCM simulations of AR5 of the IPCC, and on the conclusions drawn from the CGCM projections described in AR4.

The Southern African region is projected to experience a general increase in the number of years with below-normal rainfall, although a decrease in dry years is also plausible over the central interior regions. The analysis of CGCM simulations reveal that an increase in extreme wet years over the regions is also plausible, that is, climate variability over the region is projected to increase. In the case of the Limpopo river basin (a DEWFORA case study area), the regional projections are particularly robust in indicating an increase in below-normal rainfall years. The Limpopo basin has been shown to be the part of the African continent that experiences the highest frequency of heat-waves under present-day climate, and drastic increases in heat-wave frequencies are projected for the basin, for both the mid- and far-futures. In fact, drastic increases in heat-wave frequencies are plausible over large parts of southern Africa by the end of the century. Most of the region is consistently projected to also experience an increase in the frequency of high fire danger days.

There is a consistent and robust message in the different downscaling exercises performed of East and tropical Africa experiencing a decrease in the number of years with below-normal rainfall. The CGCM simulations analysed confirm this result, also indicating an increase in the number of wet years for the region, and reduced rainfall variability. These results are also valid for the DEWFORA case study region of the Blue Nile river basin. Heat-waves do not occur over much of the tropics under present-day conditions, due to the tropics being prone to frequent convection. However, under future anthropogenic forcing, critical temperature thresholds over the region are being exceeded in response to general regional warming, resulting in an increasing frequency of occurrence of heat-waves over the region. The number of high fire danger days is consistently projected to increase over these regions.

More uncertainty surrounds the projected futures of the number of years with below-normal rainfall over West Africa, including the DEWFORA case study region of the Niger basin. A mixed signal is projected, including increases and decreases in the number of years with below-normal rainfall. However, further to the north over North Africa and its Mediterranean coast, another robust signal exists in the projections. These regions are projected to see drastic increases in the number of years with below-normal rainfall, and a decrease in wet years. Signals of drying and more years of below-normal rainfall are also valid for the DEWFORA case study of the Oum-er-Rbia basin. These North African regions are also robustly projected to experience drastic increases in heat-wave frequencies during the 21st century.

Given the ample evidence of plausible increases in the frequency of occurrence of years of below-normal or above-normal rainfall over much of the continent, and the robust signal of heat-wave frequencies increasing over Africa under climate change, the skilful projection of these quantities at seasonal timescales may be expected to become more important. These aspects were explored in some detail over the Limpopo river basin, a case study region with a long history of quality atmospheric observations that allow for in depth model verification studies. It was shown that the state-of-the-art ECMWF seasonal forecasting system can skilfully predict the intra-seasonal variability of heat-waves and spells over the region, at seasonal time-scales. This is an encouraging result, indicating the potential of skilful seasonal forecasts as an adaptation mechanism to climate change.

TABLE OF CONTENTS

LIST OF FIGURES

1. INTRODUCTION

Large parts of the African continent are located in the subtropics, polewards of the tropical region where the Inter-tropical Convergence Zone (ITCZ) brings abundant rainfall, but also equator-wards of the rain-bringing frontal systems of the high-latitudes. Over these parts of the continent, the climate is generally semi-arid and rainfall is highly variable. This variability also implies sporadic rainfall failures and the occurrence of drought. The Sahel region in sub-tropical North Africa has suffered some of the continent's most severe droughts of the last five decades, for example, and sub-tropical southern Africa is vulnerable to the occurrence of severe droughts during El Niño years. In fact, the El Niño Southern Oscillation (ENSO) signal in Africa also extends further to the north, to East Africa, which often experiences drought during La Niña years. Additionally, the pats of West and East Africa that experience monsoon rains are vulnerable to the failure, or late arrival, of these rains. In East Africa, including the Horn of Africa, these different sources of climate variability can be the cause of devastating droughts.

Superimposed on this natural variability, the African continent is thought to be highly vulnerable to anthropogenically induced climate change (e.g. Meadows, 2006). The rate of warming over the continent is robustly estimated to be in the order of 1.5 times the global mean rate of temperature increase (Christensen et al., 2007), according to the coupled global climate model (CGCM) projections described in Assessment Report Four (AR4) of the Intergovernmental Panel on Climate Change (IPCC). It seems plausible for large parts of subtropical Africa, including southern Africa and the northern Sahara, to become drier within this generally warmer climate, whilst tropical and East Africa are robustly projected to become wetter (e.g. Christensen et al., 2007; Engelbrecht et al., 2009; DEWFORA D3.4). These changes in African climate may be expected to have wide-ranging implications, including largely negative impacts on agriculture (e.g. Thornton et al., 2011), water security and the abundance and distribution of pests and diseases (e.g. Olwoch et al., 2008).

Of particular interest in this component of the research of FP7 project DEWFORA, is the extent to which enhanced anthropogenic forcing may impact on the frequency, duration and severity of droughts over the African continent. Previous research, including that performed as part of DEWFORA, has provided evidence that rainfall decreases are plausible over both southern Africa and North Africa under climate change, largely in response to the strengthening of the subtropical high-pressure belt and the poleward displacement of the westerly winds (e.g. Seidel et al., 2007; Engelbrecht et al., 2009; DEWFORA D3.4). The DEWFORA case study region of the Limpopo river basin in Southern Africa, for example, displays a particularly strong signal of drying in regional projections of future climate change performed as part of the project - consistent with the projections of most CGCMs for this region (e.g. Christensen et al., 2007). Rainfall decreases over the Limpopo basin have been shown to result partially from increased subsidence, and the displacement of the tracks of tropical lows and cyclones to the north (Malherbe et al., 2013). Such changes would also be consistent with the more frequent occurrence of dry spells and heat waves over the region. The general expansion of the tropical belt under climate change (e.g. Seidel et al., 2007) and strengthening of monsoon circulation over East Africa under climate change may conversely imply generally wetter conditions and a decrease in the frequency of drought over the DEWFORA case studies of the Blue Nile and Niger (see Engelbrecht et al., 2013). Indeed, hydrological modelling performed as part of DEWFORA has pointed out that increased streamflow under climate change is plausible over both the Blue Nile and Niger basins (Fournet et al., 2013). However, for the fourth DEWFORA case study region of Oum-er-Rbia in Mediterranean North Africa, the northward displacement of the westerlies may imply both rainfall reductions and the increased occurrence of drought. The purpose of the research presented in this particular DEWFORA deliverable, is to explore in some detail the projected futures of metrics that are indicative of drought, such as the dry spells, heat waves and precipitation indices, with particular emphasis on Africa and the DEWFORA case study regions. High-resolution projections of climate change over Africa performed as part of the

DEWFORA research are analysed for this purpose, in combination with the analysis of projections of CGCMs.

With the seasonal forecasting of drought over Africa being a key theme within DEWFORA, potential increases in the importance of seasonal forecasting within the context of a changing climate, are also explored as part of this deliverable. Indeed, if climate change is to lead to a more variable climate system and the more frequent occurrence of extreme droughts, floods and heat waves, it will become even more important to have available seasonal forecasting systems that can skilfully predict such events. The Limpopo river basin of DEWFORA is selected as a case study to explore these aspects in detail within the current report. This region was selected due to the relatively dense network of weather stations (compared to the other DEWFORA case study regions) that facilitates model verification studies, but also because of the strong climate-change signal (significant drying and drastic warming) that is present in regional mode projections of climate change over this region. This component of the research relies on state-of-the-art high-resolution projections of future climate change over this region, performed as part of DEWFORA, in combination with a state-of-the-art seasonal forecasting system at the European Centre for Medium Range Weather Forecasting (ECMWF).

2. PROJECTIONS OF THE CHANGING ATTRIBUTES OF DROUGHT OVER AFRICA UNDER CLIMATE CHANGE

2.1 DEWFORA REGIONAL MODEL PROJECTIONS AND EXPERIMENTAL DESIGN

2.1.1 The conformal-cubic atmospheric model

The high-resolution (regional) projections of future climate change described in this component of the report were derived at the Council for Scientific and Industrial Research (CSIR) in South Africa, using the conformal-cubic atmospheric model (CCAM) developed by the Commonwealth Scientific and Industrial Research Organisation (CSIRO) in Australia (McGregor, 1996, 2005a, 2005b; McGregor and Dix, 2001, 2008). CCAM is a variable-resolution global atmospheric model and employs a semi-implicit semi-Lagrangian method to solve the hydrostatic primitive equations. The model uses a comprehensive set of physical parameterizations. The GFDL parameterizations for long-wave and short-wave radiation are used, with interactive cloud distributions determined by the liquid and ice-water scheme of Rotstayn (1997). A stability-dependent boundary layer scheme based on Monin Obukhov similarity theory is employed (McGregor et al., 1993), together with the non-local treatment of Holtslag and Boville (1993). A canopy scheme is included, as described by Kowalczyk et al. (1994), having six layers for soil temperatures, six layers for soil moisture (solving Richard's equation) and three layers for snow. The cumulus convection scheme uses a mass-flux closure, as described by McGregor (2003), and includes downdrafts, entrainment and detrainment. CCAM may be applied at quasi-uniform resolution, or alternatively in stretched-grid mode to obtain high resolution over an area of interest. The model code has been implemented for parallel processing using Message Passing Interface (MPI) software on the computer clusters of the Centre of High Performance Computing (CHPC) in South Africa.

CCAM was applied in this project to simulate both present-day and future climate over Africa. The model is highly suitable for the purpose of regional climate modelling, due to its computational efficiency and variable-resolution formulation that allows great flexibility in downscaling CGCM data, through the application of a multiple nudging technique (McGregor, 2005b; Thatcher and McGregor, 2009, 2010). The model's ability to simulate the present-day characteristics of regional climate has earlier been investigated rigorously over southern Africa (e.g. Engelbrecht et al., 2009; Landman et al., 2009; Engelbrecht et al., 2012) and for various other climatological regions (e.g. Nunez and McGregor, 2007; Lal et al., 2008).

In order to obtain the ensemble of regional projections of climate change, the model was forced with the bias-corrected sea-surface temperature (SST) and sea-ice output of six

different CGCMs used in AR4 of the IPCC, for the period 1961-2100. The CGCMs downscaled are:

- GFDL-CM2.0 [Version 2.0 CGCM of the Geophysical Fluid Dynamics Laboratory (GFDL) of the National Oceanic and Atmospheric Administration (NOAA) in the United States];
- GFDL- CM2.1 [Version 2.1 CGCM of the Geophysical Fluid Dynamics Laboratory (GFDL) of the National Oceanic and Atmospheric Administration (NOAA) in the United States];
- ECHAM5/MPI-Ocean Model [The CGCM from MPI in Germany];
- UKMO-HadCM3 (The Met Office Third Hadley Centre Coupled Ocean-Atmosphere GCM - United Kingdom);
- MIROC3.2-medres (Model for Interdisciplinary Research on Climate 3.2, medium resolution version, of the Japanese Agency for Marine-Earth Science and Technology);
- CSIRO Mark3.5 (The version 3.5 CGCM of the Commonwealth Scientific and Industrial Research Organisation in Australia).

All six of the projections performed are for the A2 emission scenario of the Special Report on Emission Scenarios (SRES). A multiple-nudging strategy was followed, by first integrating CCAM globally at quasi-uniform C48 resolution (about 200 km in the horizontal), forcing the model with the SSTs and sea-ice of each host model. In a second phase of the downscaling, CCAM was integrated in stretched-grid mode over Africa at a resolution of about 50 km in the horizontal. The higher resolution simulations were nudged within the quasi-uniform simulations, through the application of a digital filter using a 4000 km length scale. More details of the experimental design are provided by Engelbrecht et al. (2013). An important feature of the simulations is the use of bias-corrected SSTs. A problem common to almost all CGCMs, is the existence of the “cold tongue” bias along the equatorial Pacific. This bias leads to significant distortions of atmospheric flow patterns over the equatorial Pacific in the host CGCMs (e.g. Katzfey et al., 2009; McGregor et al., 2011). The use of bias-corrected SSTs in the simulations described here avoids these distortions in the simulated atmospheric flow, and makes feasible more realistic simulations of the global and also African climate.

2.1.2 Bias-correction procedure

Both CGCMs and RCMs are known to display systematic errors (biases) in their simulations of present-day climate attributes. For some applications (e.g. hydrological modelling) and before analysing certain aspects of the projected climate-change signal (e.g. heat wave days) it is essential to first remove systematic errors from the model simulations. For example, if a model systematically overestimates rainfall, direct application of the raw model data to hydrological modelling would lead to an unrealistic depiction of the hydrological cycle by the hydrological model.

A simple bias-correction procedure was applied in this research. First, the CRU TS3.1 data set of the Climatic Research Unit (CRU) was used to calculate the monthly climatologies for the variables of average daily rainfall, minimum temperature, maximum temperature, minimum relative humidity and maximum relative humidity, for the period 1961-1990. For each of the six downscalings performed, the simulated monthly climatologies were calculated for the same period. These were then used to calculate the monthly model biases (separately, for each downscaling). A bias-corrected version of each downscaling was subsequently obtained, by subtracting for each day in the simulation the relevant monthly bias - for each of the variables under consideration. In the case of rainfall, the

overestimation/underestimation was expressed as a percentage, and daily rainfall totals were corrected with an appropriate fraction (rather than to subtract the relevant monthly bias). This bias-correction procedure results in the 1961-1990 climatology for each of the six downscalings to be exactly that of CRU TS3.1, however, the inter-annual variability and daily variability remains that of the downscaled simulation.

2.2 REGIONAL MODEL PROJECTIONS OF THE CHANGING ATTRIBUTES OF DROUGHTS, HEAT WAVES AND HIGH FIRE DANGER DAYS OVER AFRICA

2.2.1 Years of below-normal rainfall in present-day and future climates

It is conventional to issue seasonal forecasts in the form of probabilistic statements of rainfall to be in either of the categories below-normal, near-normal or above-normal. The categories are usually constructed from ranking a specific time-series of (seasonal) rainfall totals in order of magnitude, to find the required set of terciles. Each member of an ensemble of seasonal forecasts is then associated with one of these categories, in order to construct the probabilistic forecast. A similar procedure is followed here, in order to determine whether years of below-normal rainfall, as defined by present-day time series, may be expected to decrease or increase under climate change. More specifically, for each of the six regional model projections described in Section 2.1, the period 1961-1990 was used to define the below-normal category of rainfall for each grid-point in the model domain over Africa. Following the procedure described above, ten years in the time-series 1961-1990 are associated with the below-normal category for each grid-point in the model domain (and for each of the ensemble members). It was subsequently determined whether the mid-future (2041-2070) and far-future (2071-2100) periods exhibit increases or decreases in the number of years characterised with below-normal rainfall (in terms of the below-normal category associated with present-day climate). The results obtained using the procedure outlined above are displayed in Figures 2.1 and 2.2, for the mid- and far-futures, respectively. It may be noted that the general patterns of the projected changes are similar for mid-and far-future periods, but with the amplitude of the changes strengthening over time. A number of climate change signals that are robust across the ensemble of downscalings can be discerned from the figures.

The Southern African region is projected to experience a general increase in the number of years with below-normal rainfall. However, 3 of these ensemble members indicate that it is plausible for below-normal rainfall years to occur less frequently over the central interior of the Southern African region. This is consistent with some downscalings indicating increases in rainfall totals over these regions (Engelbrecht et al., 2013). In the case of the Limpopo river basin, a DEWFORA case study region, the majority of ensemble members are projecting an increase in the number of years of below-normal rainfall, although a decrease in this number also represents a plausible (but less likely) future. Most downscalings consistently indicate a decrease in rainfall totals for the Limpopo river basin, consistent with a projected northward displacement of tropical cyclone and low tracks over the southwestern Indian Ocean (Malherbe et al., 2013).

There is a consistent and robust message across the ensemble members of East and tropical Africa experiencing a decrease in the number of years with below-normal rainfall, which is consistent with most ensemble members projecting increases in rainfall totals over these regions (Engelbrecht et al., 2013). This signal also holds for the Blue Nile basin (a DEWFORA case study region), and is likely to favour increases in streamflow over this region (Fournet et al., 2013). More uncertainty surrounds the projected futures of the number of years with below-normal rainfall over West Africa, including the DEWFORA case study region of the Niger basin. A mixed signal, of both increases and decreases in the number of years with below-normal rainfall, is projected. However, further to north over North Africa and its Mediterranean coast, another robust signal exists in the projections. These regions are projected to see drastic increases in the number of years with below-normal rainfall. The projected changes are consistent with the projected poleward displacement of the westerly

winds, and general reductions in rainfall totals projected for these regions. Signals of drying and more years of below-normal rainfall are also valid for the DEWFORA case study of the Oum-er-Rbia basin.

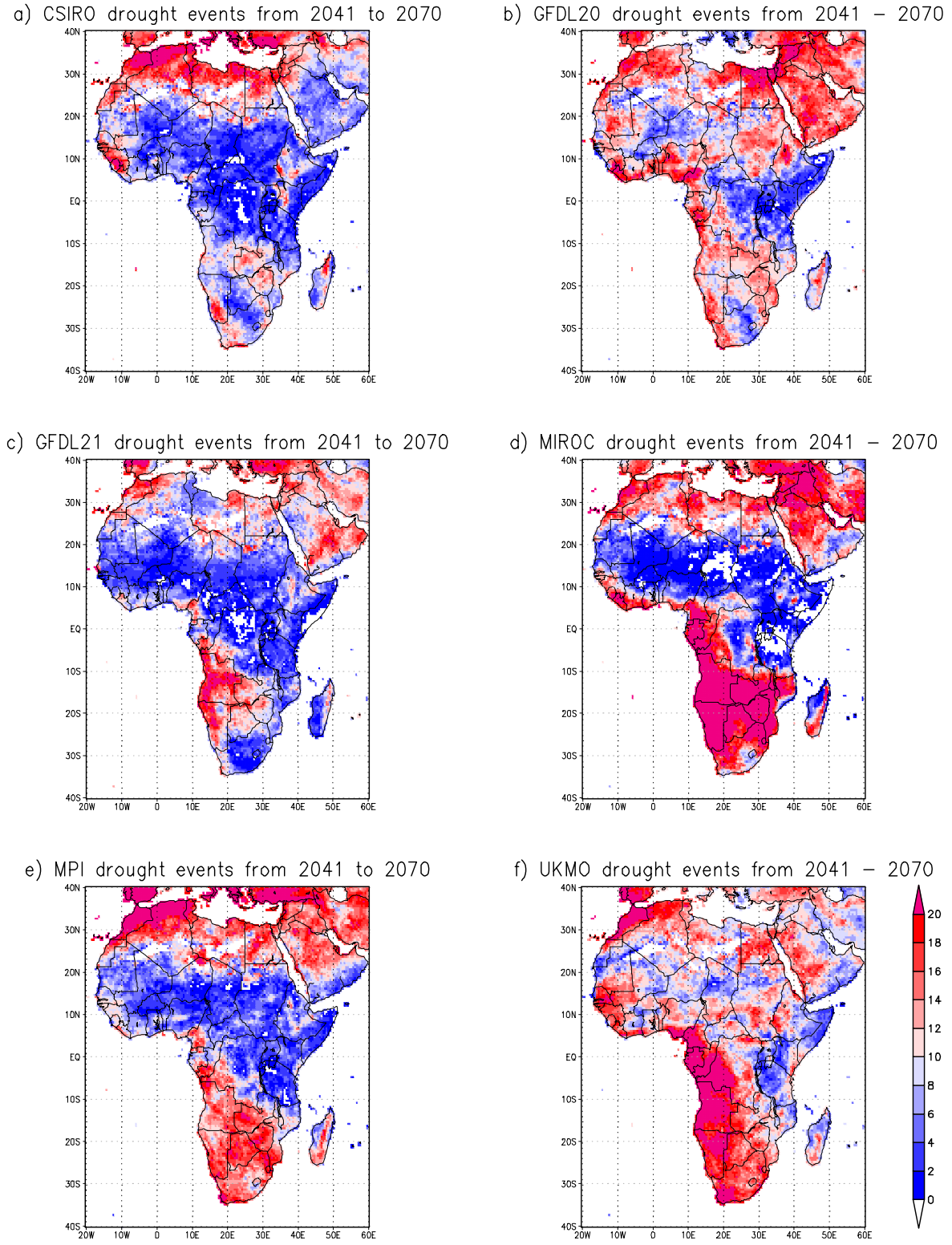

Figure 2.1. Projected number of years with rainfall in the below-normal category, for the period 2041-2070, across the African continent. The period 1961-1990 was used to construct the terciles of below-normal, near-normal and above-normal rainfall.

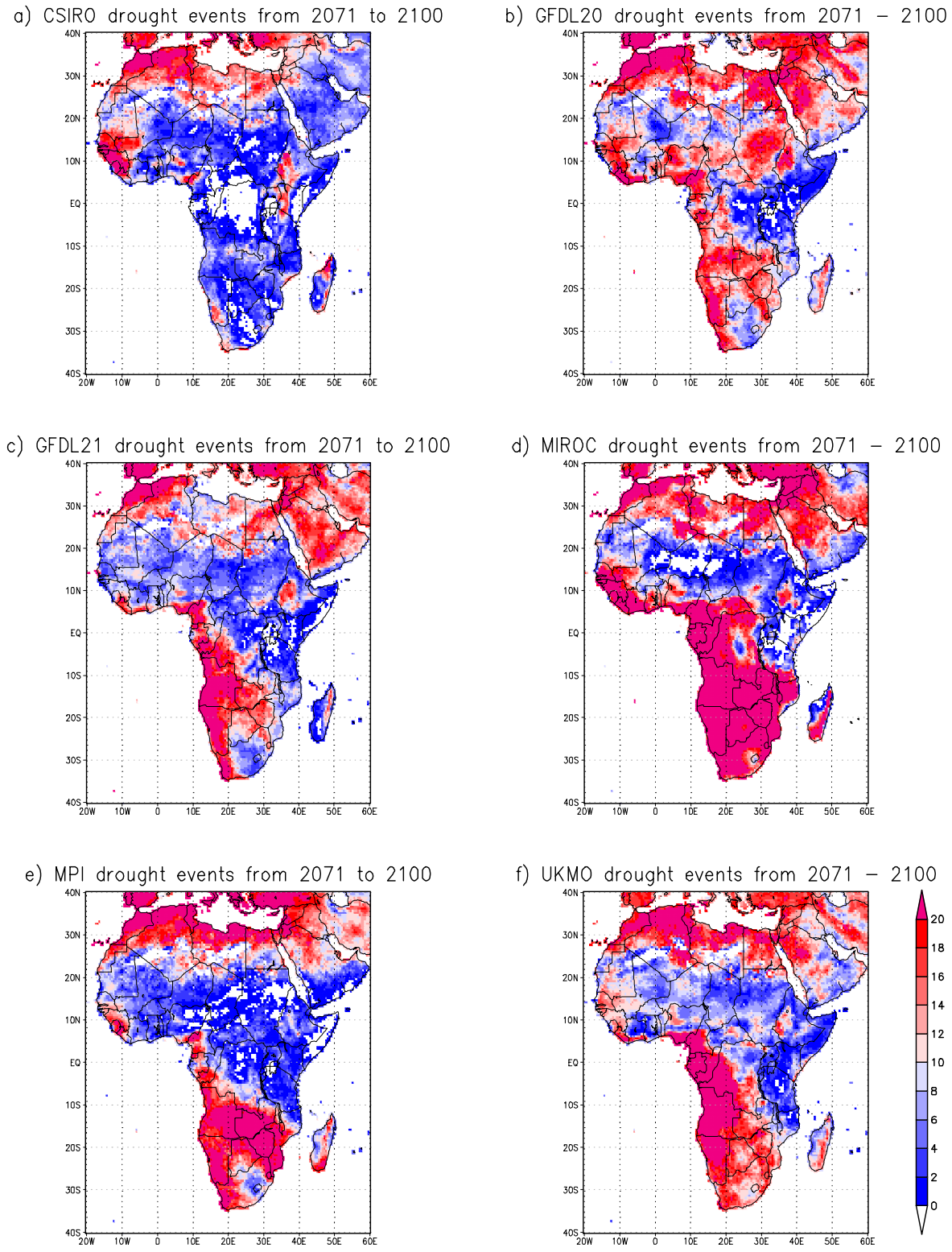

Figure 2.2. Projected number of years with rainfall in the below-normal category, for the period 2071-2100, across the African continent. The period 1961-1990 was used to construct the terciles of below-normal, near-normal and above-normal rainfall.

2.2.2 Projected changes in heat-wave frequencies over Africa

Over sub-tropical Southern Africa and North Africa, heat-waves tend to occur in association with periods of sustained anti-cyclonic circulation and subsidence. That is, heat waves occur when mid-level high-pressure systems dominate the circulation for a sustained period of a few days to weeks. Over Southern Africa, dry El Niño summer seasons are also associated with a higher-than-normal frequency in the occurrence of heat waves. That is, heat-waves represent an important mechanism through which seasons of drought impact negatively on agriculture and other sectors at the intra-seasonal time-scale. It is also noteworthy that the maize crop, which is of key importance to subsistence and commercial farming across the African continent, is projected to decrease drastically in yield if continental temperatures are to rise drastically (e.g. Thornton et al., 2011). The maize crop is vulnerable in particular to the occurrence of extreme temperature events. The projected drastic rises in surface temperature over Africa (e.g. Engelbrecht et al., 2013) is therefore a source of particular concern, as it represents not only changes in average temperatures – but superimposed on these changes, an increased frequency in the occurrence of heat-waves that may lead to critical temperature thresholds being exceeded more often. Indeed, there is evidence of the tropical belt widening (Seidel et al., 2007) and the subtropical high-pressure belt strengthening over Southern and North Africa under climate change (e.g. Engelbrecht et al., 2009). The latter large-scale change has been shown to occur in association with the more frequent-formation of mid-level highs, and possibly heat-waves, over the subtropics. These aspects are explored in more detail in the current subsection, using the set of high-resolution regional projections described in Section 2.1. The World Meteorological Organisation (WMO) definition of a heat-wave is applied in the research: an event where the maximum temperature at a location exceeds the average temperature of the warmest month at that location with 5 °C or more, for a period of at least 3 days.

The simulated annual average number of heat waves occurring over Africa during the period 1961-1990 are shown in Figure 2.3, for each of the downscalings described in Section 2.1. The highest frequency of heat waves (about 60 over the 30-year period) are simulated to occur in the Limpopo river basin of Southern Africa. Generally, Southern Africa and North Africa are the regions with the highest frequencies of heat waves. These are regions in the sub-tropical high pressure belt, prone to the formation of subsidence and mid-level highs. Large parts of tropical Africa and the Sahara are simulated not to experience heat waves in present-day climate. This is due to the high threshold temperatures not being exceeded for sufficiently long periods to satisfy the heat-wave definition.

The projected increase in the number of heat-waves across the African domain are shown in Figures 2.3 and 2.4, for the mid- and far-futures, respectively. The highest increases are projected for the regions most prone to heat-waves in present-day climate – the Limpopo river basin and North Africa. Over the Limpopo basin, drastic increases are projected, with some parts of the basin projected to experiencing more than 200 events during the mid-future period 2041-2070. For the far-future, it is projected that a large part of the southern African region is to experience more than 240 heat wave events. Heat waves are also projected to start occurring over the tropics by the mid-future. This is the result of the critical threshold temperature (defined be the present-day warmest month) being exceeded satisfying the heat-wave definition, due to the systematic increases in the background state temperatures. Heat wave- frequency increases are also projected to be relatively high over North Africa, including the DEWFORA case study area of the Oum-er-Rbia catchment. The projected patterns of changing heat-wave frequencies are robust across the ensemble of regional projections, similar to the projected temperature signal over Africa (Engelbrecht et al., 2013). With the underlying circulation changes driving the heat-wave signal well understood, it may be regarded as an actionable signal – and probably one of the most important and high-impact aspects of future climate change over Africa.

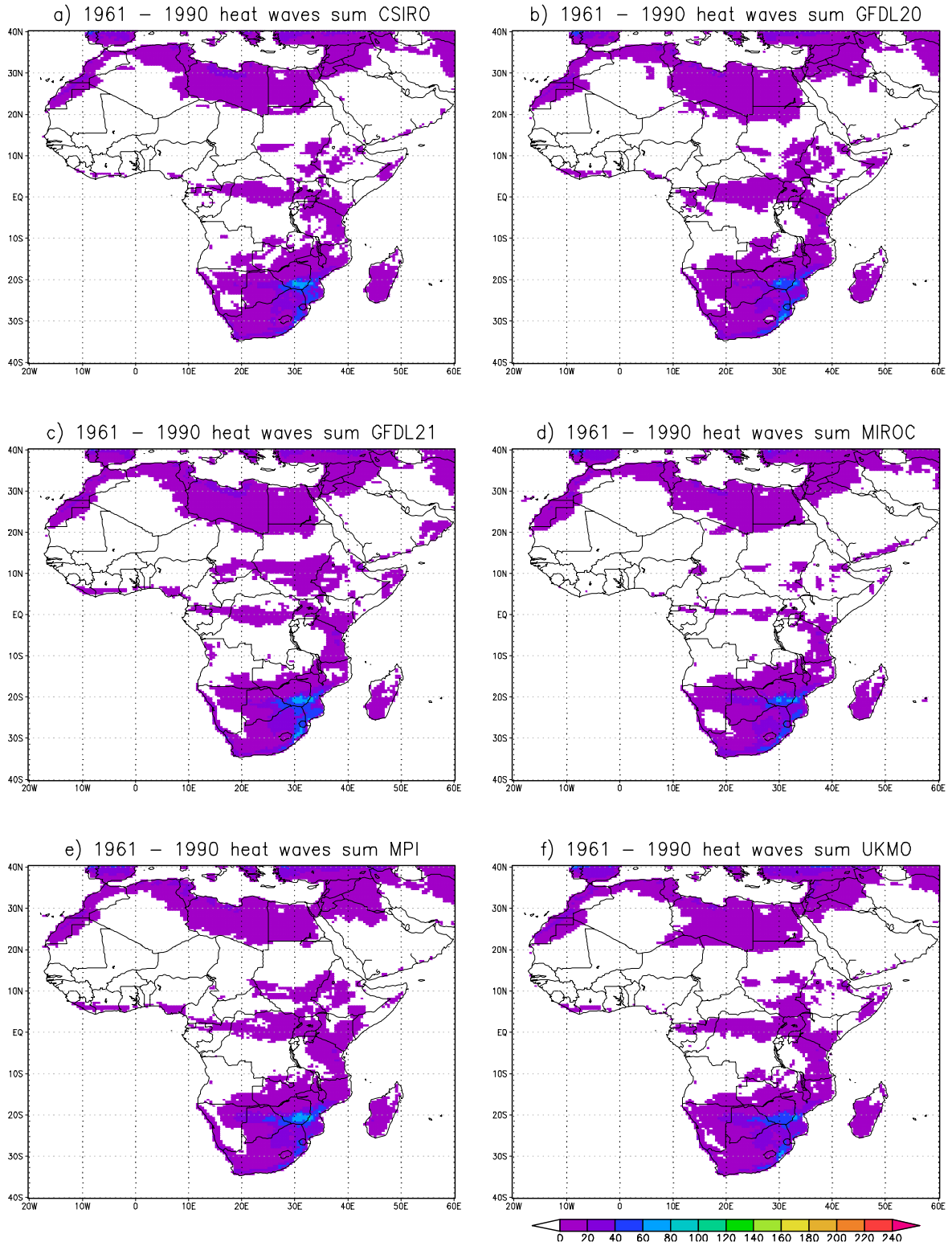

Figure 2.3. Simulated number of heat-wave events for the mid-future period 1961-1990, for the 6 different CCAM projections.

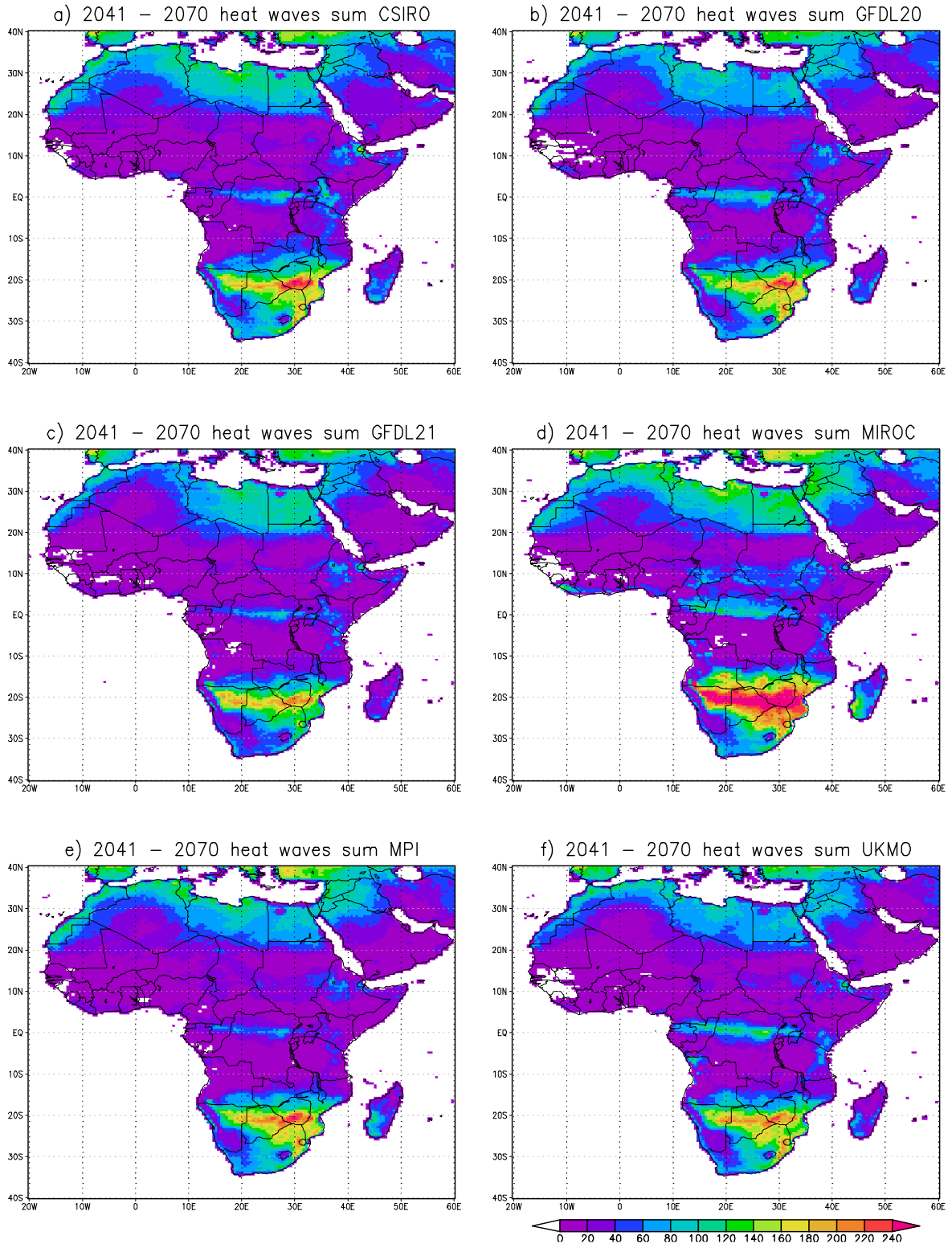

Figure 2.4. Projected number of heat-wave events for the mid-future period 2041-2070, for the 6 different CCAM projections.

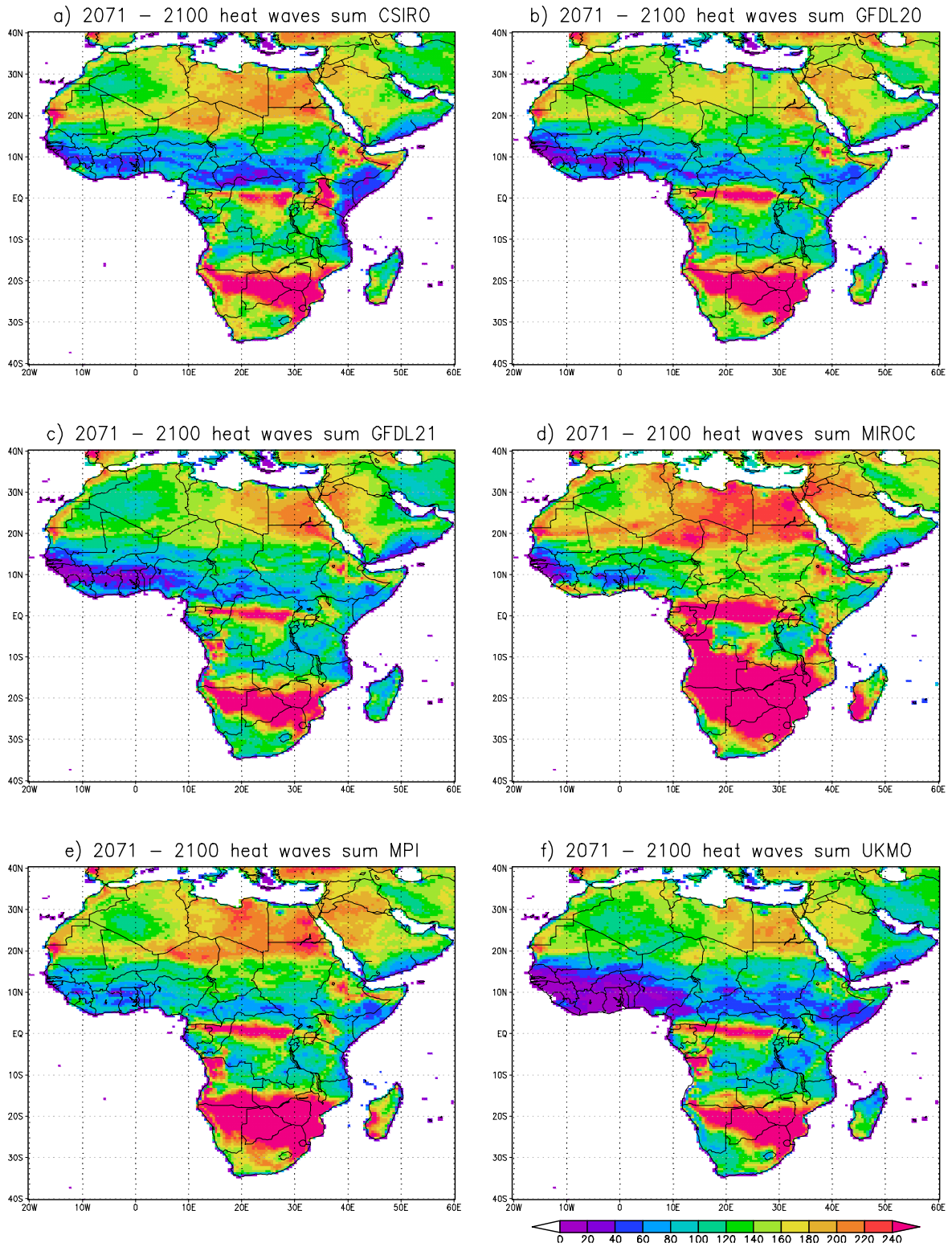

Figure 2.5. Projected number of heat-wave events for the far-future period 2071-2100, for the 6 different CCAM projections.

2.2.3 Projected changes in the number of high fire-danger days over Africa

Temperatures are projected to rise drastically over Africa during the 21st century under strong emission scenarios such as the SRES A2 scenario (e.g. Engelbrecht and Bopape, 2011; Engelbrecht et al., 2013). The most drastic temperature increases are projected for the sub-tropical parts of the continent, and are simulated to occur in association with the strengthening of the subtropical high pressure belt over Southern Africa and North Africa and the poleward displacement of the westerly wind regime (and cold fronts). These circulation changes imply that it is plausible for large parts of Southern Africa and North Africa to become generally drier under future climate change (see Section 2.2.1). Generally drier and warmer conditions over the subtropics of Africa are likely to be associated with increased fire risk. This section of the research makes use of a fire index to objectively project changes in the frequency of occurrence of high fire danger days over Africa. The index used is the McArthur Forest Fire Danger Index (FFDI), and its standard formulation (e.g. Dowdy et al. 2010) is applied. The FFDI depends on the calculation of a drought index defined by Keetch and Byram (1968), taking into account the required corrections pointed out by Alexander (1990). The FFDI has been used extensively to study fire risks over South Africa and Australia (e.g. Van Wilgen et al., 2010), and is applied here to the six high-resolution projections of future climate change over Africa (described in Section 2.1).

The simulated the annual averages across the continent, of the number of days when the FFDI is rated as high, very high or extreme (FFDI > 12), calculated for the period 1961-1990, are shown in Figure 2.6 for each of the six ensemble members. The fire danger climatologies of the six downscalings are very similar – this may be attributed to the bias-correction procedure, which has effectively transformed the monthly climatologies of all the downscalings to that of the CRU data (see Section 2.1). The highest values of high fire danger days are simulated to occur over the sub-tropics, including Southern Africa, the Horn of Africa, the Sahel region and the Sahara. Over these regions as many as 90 high fire danger days are simulated to occur annually, with values exceeding 140 days per year over some regions. It may be noted that although the number of high fire danger days are simulated to reach maximum values over regions such as Namibia and the Sahara, the vegetation burning capacity of these regions is low, or insignificant. The lowest numbers of high fire danger days, less than 20 days per year, are simulated over the tropics with its high frequency of rain days.

Figure 2.7 shows the model projected changes in the number of days per year when the FFDI value is rated as high, very high or extreme (FFDI > 12), for the mid-future period 2041-2070, relative to the baseline period 1961-1990. Figure 2.8 shows the same result, but for the far-future period 2071-2100. The downscaled models project a robust pattern of drastic increases in the FFDI and high fire danger days over Southern Africa, tropical Africa, Madagascar and the Mediterranean coasts of North Africa and South Africa - for the mid- and far-future time-slabs 2071-2100 relative to the baseline period. High fire danger days are projected to increase by 40 days or more per year over large parts of these regions, for the far-future period. These increases are driven by the drastic rises in surface temperature over these regions. However, over the warm deserts of Africa, namely the Sahara and Namib, as well as over large portions of the Sahel, the ensemble of downscalings project a robust pattern of decreasing high fire danger days. These are the warmest parts of the African continent, and even in the baseline climate the critical temperature thresholds that trigger high fire danger days are often exceeded. Further temperature increases under the enhanced greenhouse effect therefore have a relatively small effect on increasing the FFDI over these regions. However, with increases in the number of convective rainfall events projected for these regions (Engelbrecht et al., 2013), the number of high fire danger days are projected to decrease. This may be of little consequence to the desert areas, where the vegetation burning capacity is low – at least for present-day vegetation patterns. It may be an

important result for the Sahel region, however, due to the complex interactions between fire and the African savanna.

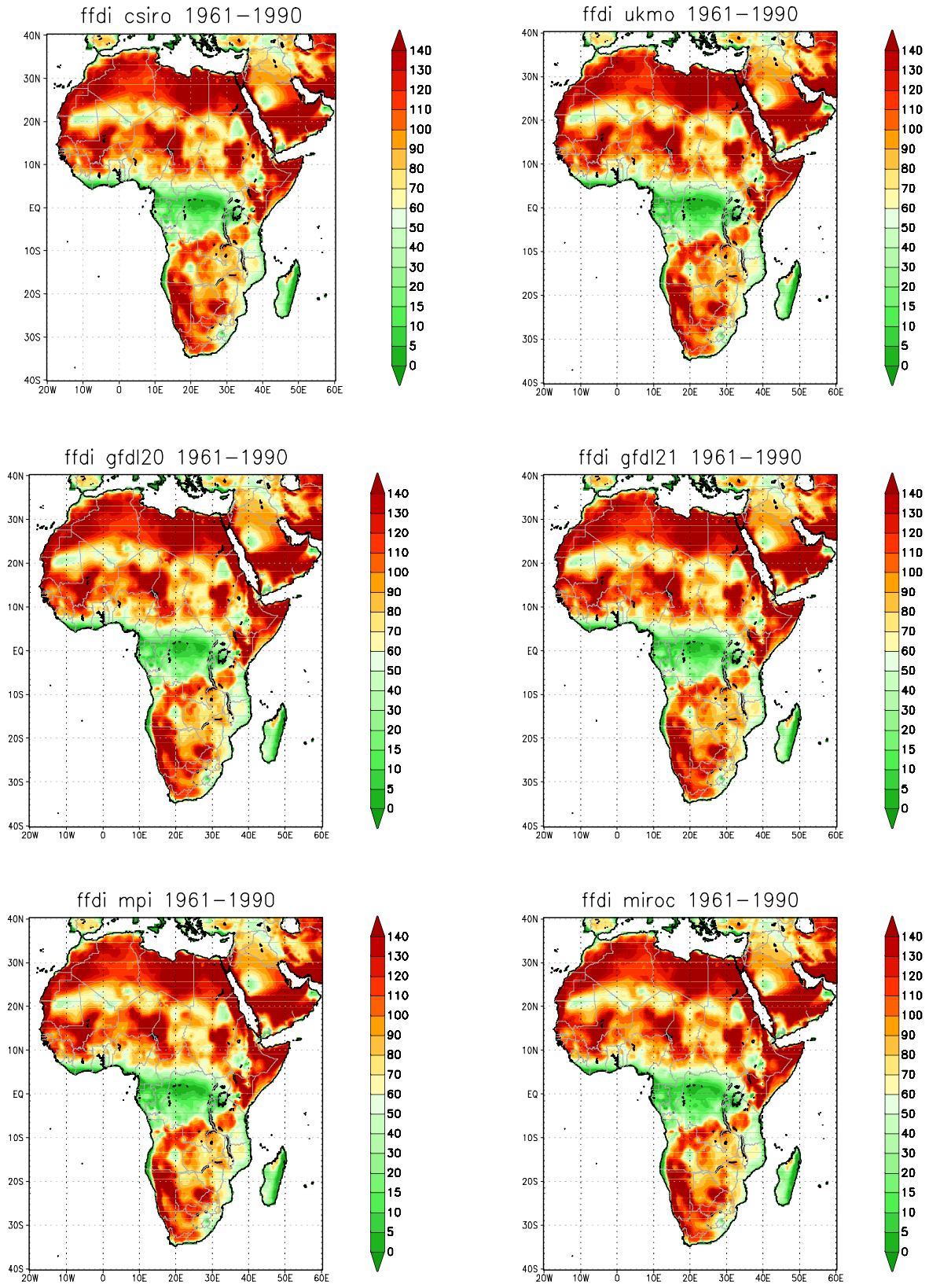

Figure 2.6. Regional model simulations of the number of high fire danger days occurring annually over Africa (averaged over the period 1961-1990).

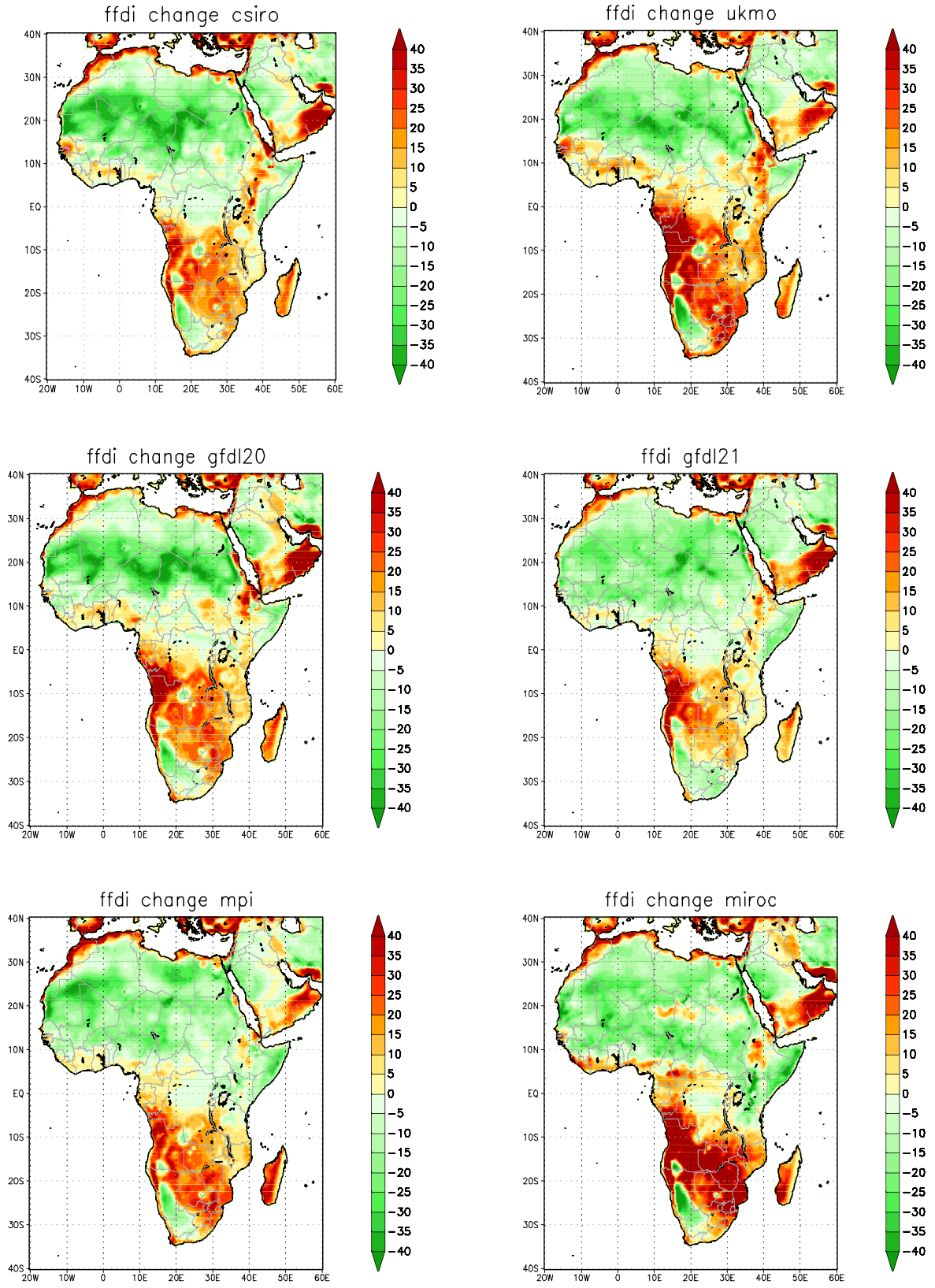

Figure 2.7. Regional model projections of change in the annual number of high fire-danger days over Africa, for the period 2041-2070 relative to 1961-1990.

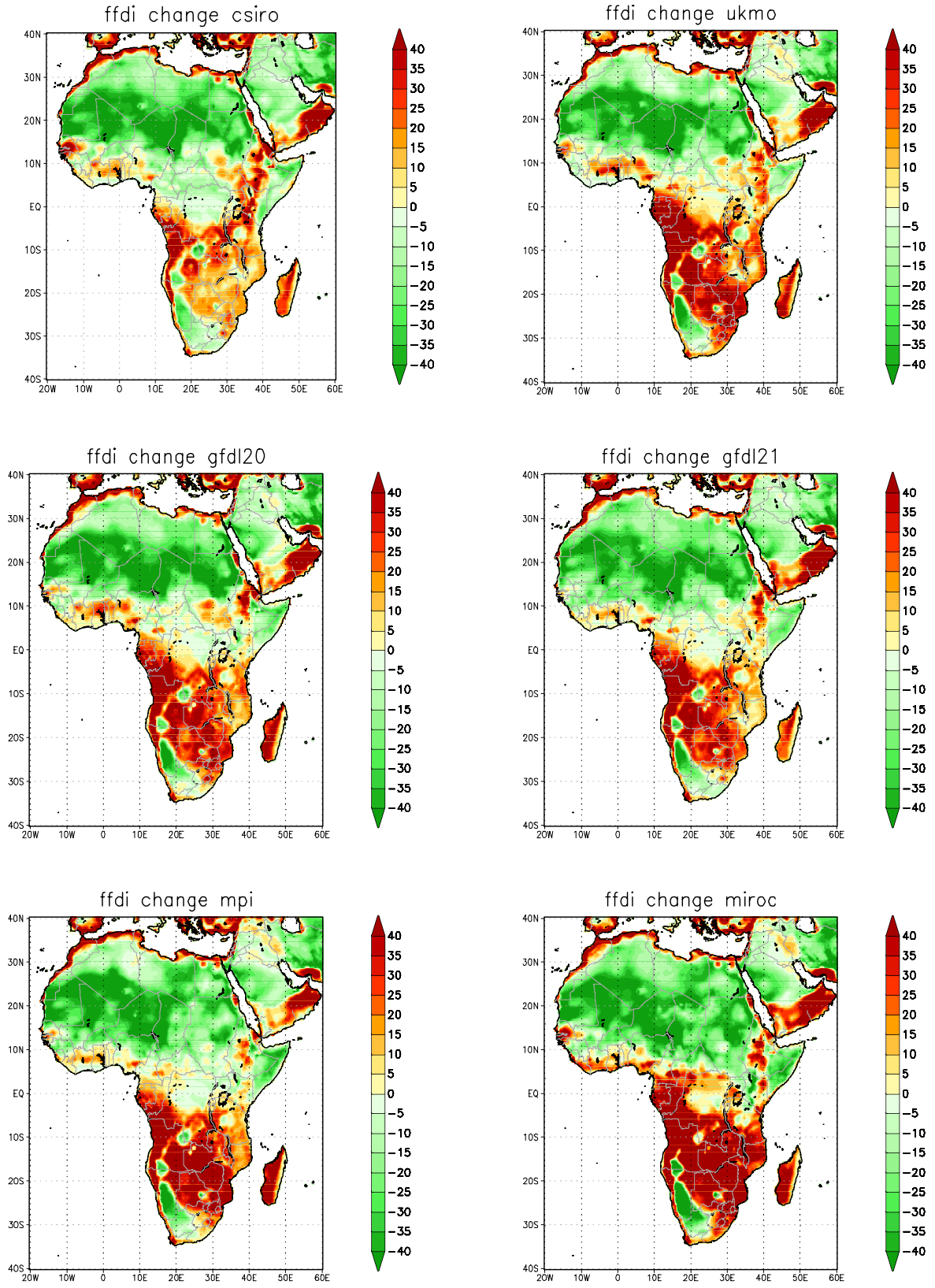

Figure 2.8. Regional model projections of change in the annual number of high fire-danger days over Africa, for the period 2071-2100 relative to 1961-1990.

2.3 CGCM PROJECTIONS OF THE CHANGING OCCURRENCE OF DROUGHT OVER AFRICA UNDER CLIMATE CHANGE USING THE STANDARDIZED PRECIPITATION INDEX

2.3.1 Introduction

Changes in the probability of occurrence of extreme dry and wet years over Africa under climate change are analysed in this section, using the Standardized Precipitation Index (SPI) as a metric of drought. A projection of future climate from the CNRM-CM5 CGCM, for RCP 4.5, is used as the basis for the analysis. Results are also presented on projected changes in the frequency, duration and severity of droughts over Africa under climate change. The methodology applied in this component of the research report is based on that of Russo et al. (2013), which has previously been applied successfully to study drought characteristics over Europe within a changing climate.

2.3.2 Data

The analysis presented in this component of the report is based on a projection of the CNRM-CM5 CGCM, one of the global climate models that contributed to the Coupled Model Intercomparison Project Phase 5 (CMIP5) and Assessment Report Five (AR5) of the IPCC. A description of the CNRM-CM5 component models and OASIS coupler, developed at CERFACS, is provided by Voldoire et al. (2011).

The CMIP5 simulations are based on Reference Concentration Pathways (RCPs). These scenarios describe possible greenhouse-gas concentration pathways throughout the 21st century, and correspond to different radiative forcing levels by the year 2100 (e.g. Giorgi et al., 2009). In this study we selected an RCP that corresponds to a radiative forcing level of 4.5 W/m^2 (RCP4.5). This RCP roughly corresponds to the IPCC SRES emission scenario B1, and is one of the highest-priority scenarios that have been selected in CMIP5, together with RCP8.5 (which is similar to the A1B SRES scenario).

2.3.3 Standardized Precipitation Index (SPI)

The Standardized Precipitation Index (SPI) was developed by McKee et al. (1993, 1995) to provide a spatially and temporally invariant measure of the precipitation deficit (or surplus) for any accumulation timescale. It is computed by fitting a parametric Cumulative Distribution Function (CDF) to a homogenized precipitation time-series and applying an equi-probability transformation to the standard normal variable. This gives the SPI in units of number of standard deviations from the median.

Typically, the gamma distribution is the parametric CDF chosen to represent the precipitation time-series (e.g. McKee et al. 1993, 1995; Lloyd-Hughes and Saunders 2002; Husak et al. 2007) since it has the advantage of being bounded on the left at zero and positively skewed (Thom 1958; Wilks 2002). Moreover, Husak et al. (2007) have shown that the gamma distribution adequately models precipitation time-series in roughly 98% of locations over Africa. In this study we use the Maximum-Likelihood Estimation (MLE) method to estimate the parameters of the gamma distribution.

A reduction in precipitation with respect to the normal precipitation amount is the primary driver of drought, resulting in a successive shortage of water for different natural and human needs. Since SPI values are given in units of standard deviation from the standardized mean, negative values correspond to drier periods than normal and positive values correspond to wetter periods than normal. The magnitude of the departure from the mean is a probabilistic measure of the severity of a wet or dry event (Table 2.1). Since the SPI can be calculated over different rainfall accumulation periods, different SPIs allow for estimating different potential impacts of a meteorological drought:

- SPIs for short accumulation periods (e.g., SPI-1 to SPI-3) are indicators for immediate impacts such as reduced soil moisture, snowpack, and flow in smaller creeks;
- SPIs for medium accumulation periods (e.g., SPI-3 to SPI-12) are indicators for reduced stream flow and reservoir storage; and
- SPIs for long accumulation periods (SPI-12 to SPI-48) are indicators for reduced reservoir and groundwater recharge, for example.

The exact relationship between accumulation period and impact depends on the natural environment (e.g., geology, soils) and the human interference (e.g., existence of irrigation schemes). In order to get a full picture of the potential impacts of a drought, SPIs of different accumulation periods should be calculated and compared. A comparison with other drought indicators is needed to evaluate actual impacts on the vegetation cover and different economic sectors.

Definition of SPI classes and their probability of occurrence (in percent)

SPI ≤ -2	Extremely dry	2.3 %
-2 < SPI ≤ -1.5	Severely dry	4.4 %
-1.5 < SPI ≤ -1	Moderately dry	9.2 %
-1 < SPI ≤ 1	Near normal	68.2 %
1 < SPI ≤ 1.5	Moderately wet	9.2 %
1.5 < SPI ≤ 2	Severely wet	4.4 %
SPI ≥ 2	Extremely wet	2.1 %

Table 2.1. Definition of Standard Precipitation Index (SPI) classes according McKee et al (1995).

2.3.4 The relative SPI

The relative SPI is defined with respect to a reference period, in this case the 1970-2000. To compute the relative SPI, the Gamma distribution is estimated for the reference and for the future period. The two curves are then used to calculate the probability difference between future and present SPI values.

As an example, the black, red and green curves in Figure 2.9 are the CDFs fitted to the precipitation data of the present and future periods (2041-2070 and 2071–2100 respectively), which is wetter (right shifting and widening of the PDF) in a point in the Limpopo Basin and drier (left shifting of the PDF) in a point in the Moxico Province in Angola. These two points have been selected because they experience different future changes. The black curves represent the CDFs fitted to the precipitation data of the reference period (1971–2005). For the present climate, we found a value of 981 mm/yr corresponding to a standard normal value of −2 (extremely dry according to Table 2.1) in the Moxico Province. In the future climate (green line), this same amount of rain corresponds to a probability of ≈8% or, equivalently, to a standard normal value of ≈−1.2 (moderately dry). The probability of an extreme dry year (according to present-day standards) has, therefore, increased more than 3 times.

A similar procedure holds for the wet end of the distribution. For example, for the point analyzed in the Limpopo Basin (Figure 2.9 left), the precipitation that corresponds to a SPI of 2 (extremely wet) in the present climate is 1540 mm/yr, while for the future the same amount of precipitation corresponds to a probability of ≈10%.

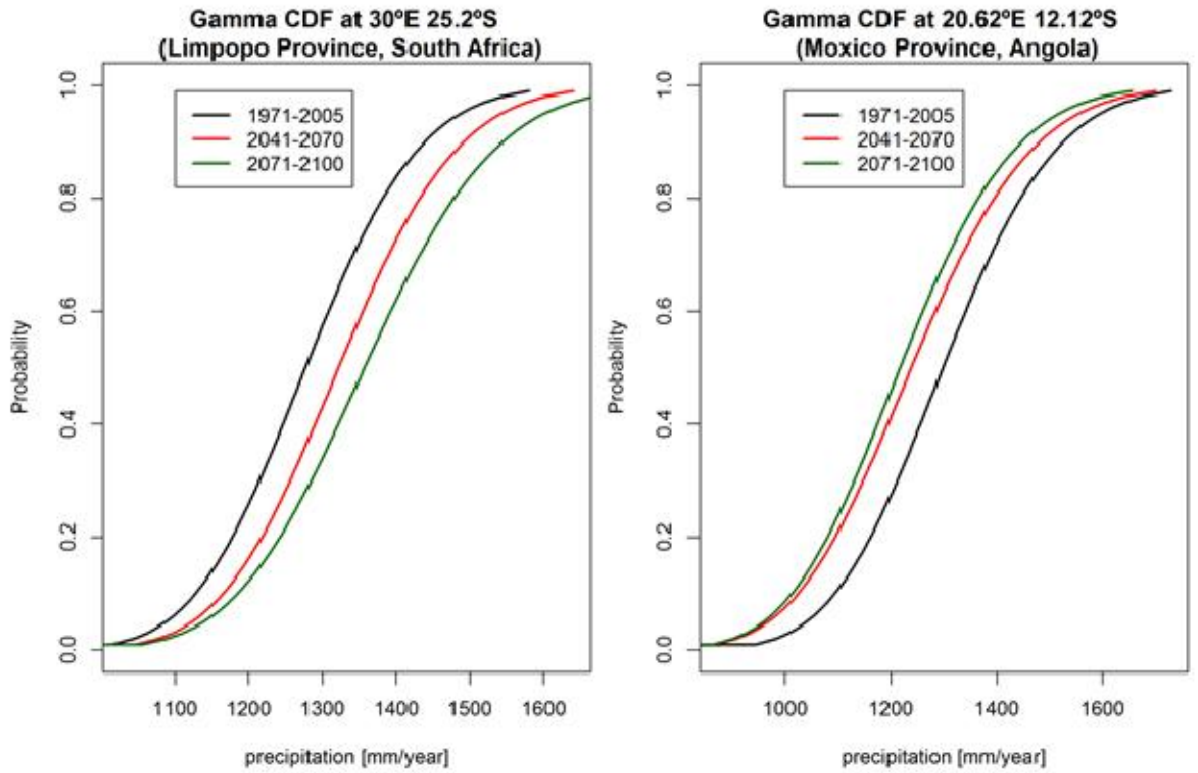

Figure 2.9. Gamma distribution at points in the Limpopo Province in South Africa (left) and in the Moxico Province in Angola (right), respectively.

2.3.5 Projected changes in the probability of occurrence of extreme dry and wet years

The CNRM-CM5 RCP 4.5 projected changes in annual rainfall totals over Africa, for the periods 2041-2070 (mid-future) and 2071-2100 (far-future), relative to the baseline period of 1971-2004, are shown in Figure 2.10. These changes are presented in terms of the differences in the 2nd and 98th percentiles, as calculated for the different climatological periods mentioned above. For both the mid- and far-futures, the 2nd and 98th percentiles indicate the same direction of change over tropical and East Africa, namely a general increase in annual precipitation. Over North Africa, a similarly robust pattern of general rainfall decreases is projected. Over Southern Africa, the 2nd percentile is indicative of drying, whilst the 98th percentile is indicative of wetting. This result suggests that years exhibiting extremely low or extremely high rainfall over Southern Africa may occur more frequently (that is, rainfall is projected to become more variable, with more years exhibiting extreme precipitation anomalies).

Mid-Future (2041-2070) projected changes in the SPI

Mid-future SPI-based projected changes in the occurrence of extreme dry year are shown in Figure 2.11 (top left). Increasing probabilities are projected mainly for the Mediterranean coast of Morocco and Algeria, the Nile basin, the whole Southern Africa region and Madagascar. The highest increases in the probability of occurrence of extreme dry years are projected for Morocco and South Africa, with values that exceed 10%. This also implies that for these regions, extreme dry years as characterised by present-day climate are projected to become the norm in the mid-future.

The probability of occurrence of extreme wet years in the mid-future is projected to increase across tropical Africa and East Africa, and also over for most of the southern Africa region

(Figure 2.12 top right). In some regions of central tropical Africa the probability is projected to increase by more than 20%.

Far-future (2071-2100) projected changes in the SPI

For the far-future the model projection displays a very similar spatial pattern than for the mid-future, but with a general increase in the amplitudes of the projected changes (Figure 2.11 bottom). The highest probabilities for the occurrence of extremely dry years are projected for West Africa (Senegal, Mauritania, Ivory Coast and Ghana).

Expected changes during the seasons

The projected changes in the probability of occurrence of extremely dry and wet seasons are shown in Figures 2.12 to 2.15, for the seasons December to February (DJF), March to May (MAM), June to August (JJA) and September to November (SON).

Most prominent are the increased probabilities of the occurrence of both wet and dry years over southern Africa across all seasons, and in particular the austral summer (DJF), increased probabilities of extreme dry seasons to occur over the Sahel and North Africa, including the Mediterranean coast during the boreal winter (JJA), and the high probabilities of an increase in wet seasons over East Africa, especially in the far-future.

Southern Africa

The Southern African region is projected to experience an increase in both extremely dry and extremely wet years, also during the important summer rainfall season DJF (Figures 2.11 and 2.4). These results may be interpreted within the context of recent findings, where decreases in summer precipitation and annual rainfall totals over southern Africa were projected (e.g. Christensen et al., 2007). The general pattern of rainfall decreases may be explained by the strengthening of the subtropical high-pressure belt over Southern Africa and its southward expansion under enhanced anthropogenic forcing (e.g. Engelbrecht et al., 2009). Also, as shown in Figure 2.14, the projections are indicative of enhanced probabilities of extreme dry winters (JJA) to occur over the winter rainfall region of the southwestern Cape of South Africa, for both the mid- and far-future. These changes are projected to occur in conjunction with strengthening of the sub-tropical high-pressure belt during winter and the consequent southward displacement of the westerly wind regime and cold fronts that bring rainfall to the winter rainfall region of South Africa (e.g. Engelbrecht et al., 2009).

East Africa

For this region the CNRM-CM5 simulation shows a general decrease in the probability of occurrence of extremely dry years under enhanced anthropogenic forcing, and a general increase in the probability of occurrence of extremely wet years. These patterns are consistent with findings from AR4 of the IPCC, which indicate that general increases in rainfall are plausible over East Africa, east of Great Lakes, and extending into the Horn of Africa (e.g. Christensen et al., 2007; Engelbrecht et al., 2009). The above described signals for wet and dry years and seasons are robust for the annual rainfall as well as for DJF and SON seasons. Increases in the intensity of the East African monsoon is the physical mechanism that is thought to be driving the rainfall changes. For the simulations presented here, the wetting signal seems to be weaker for the MAM and JJA seasons.

Tropical Africa

In the African tropics a decrease (increase) in the probability of occurrence of extreme dry (wet) events are projected for all the seasons. These changes are consistent with the projections of the CCAM ensemble depicted in the Section 2 of the report. These changes are projected to occur in conjunction with increases in tropical convection and the widening of the tropical belt (Lu et al., 2007; Seidel et al., 2007; Engelbrecht et al., 2009).

West Africa and the Sahel

Over the North African west coast an increase in the probability of occurrence of extreme dry years is projected, with consistent changes projected for most seasons. This signal is most prominent for JJA, with local extreme values in Morocco and the Atlantic coasts of Mauritania and Senegal. These changes are projected to occur in response to the systematic poleward shift of storm tracks (e.g. Christensen et al., 2007).

2.3.6 DROUGHT FREQUENCY, DURATION AND SEVERITY

Defining drought severity

It may be argued that frequency alone is not sufficient to describe drought as a hazard. In a more comprehensive way, drought phenomena may be described by their magnitude and duration, together with the frequency of their occurrence. In this section a bivariate approach to define drought hazard, using drought severity and duration derived from the SPI, is outlined.

Each period with continuous negative SPI is defined as a drought event. Cumulative SPI values of a dry event are used to measure the severity of drought event and, following McKee (1993), drought severity is defined as:

$$S = -\sum_{i=1}^{D} SPI_i \qquad 1$$

Where S is the severity and D represents the drought duration (in months) of each dry event.

Having selected SPI as the drought indicator to be used, drought can be defined as a period in which the SPI itself is continuously below a certain threshold (Table 2.1). However, definition of the time scale is required for any specific evaluation since its impacts on different socio-economic systems are dependent on the time scale.

Figure 2.16 is a frequency map showing the probability of having SPI below -1 during 1990-2010, for different aggregation periods (3, 6, 9, and 12 months). Here only small differences are observed, mostly in the Sahel, where meteorological and agricultural droughts (based on SPI3) are more likely when compared to other regions on the continent. Conversely, in central Africa (e.g. in the Democratic Republic of the Congo) more frequent hydrological droughts are associated with SPI9 and SPI12. Moreover, there exists low frequency oscillations related to drought occurrence and severity (e.g. Malherbe et al. 2012). This means that the drought hazard definition is dependent on the aggregation period analysed.

Changes in drought frequency, duration and severity were analysed using the relative SPI. In this analysis, meteorological, short term and long term droughts were be represented by SPI values computed at time scales of 1, 3 and 12 months. These aggregation periods roughly characterizes the impact that droughts can have in meteorological, agricultural and hydrological systems, respectively.

Three different parameters were chosen to characterize droughts: frequency, duration and severity. A drought event is considered here as the period in months where SPI values are below -1.0, while its severity (S) is defined as in equation 1.

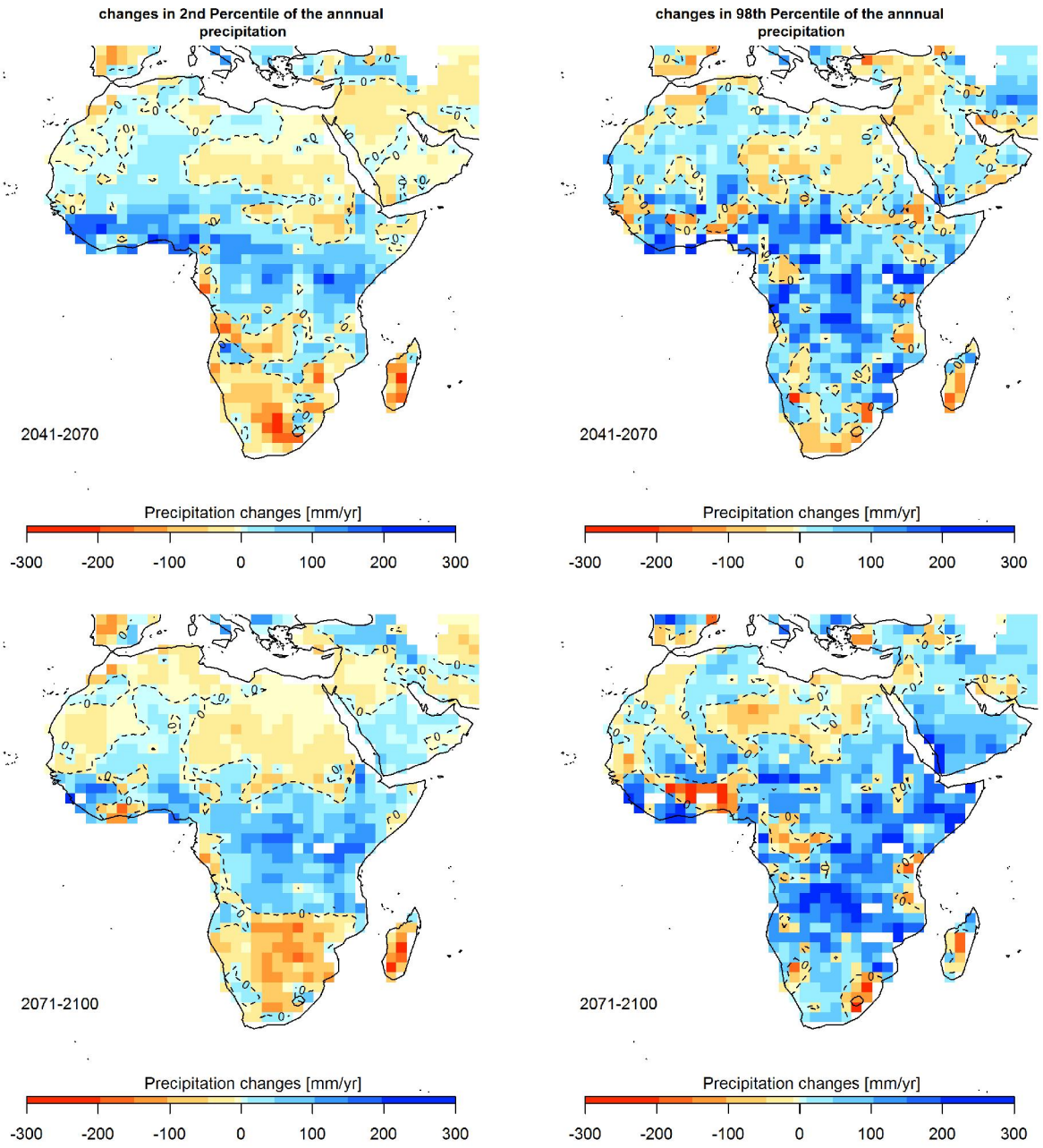

Figure 2.10. CNRM-CM5 RCP 4.5 projected changes in the 2nd (left) and 98th (right) percentiles of annual rainfall totals for the periods 2041-2070 (top) and 2071-2100 (bottom), relative to the baseline period (1971-2004).

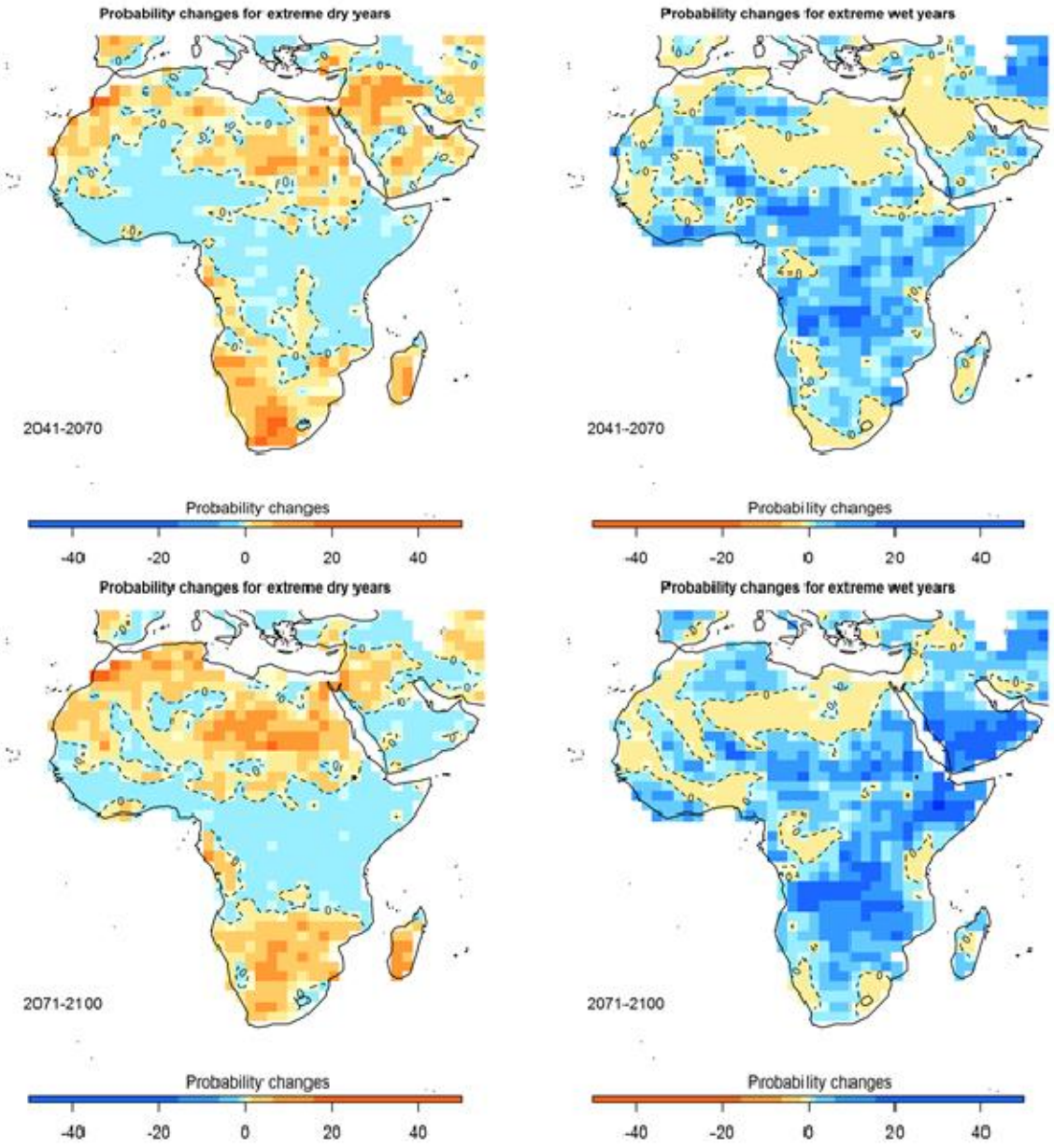

Figure 2.11. CNRM-CM5 RCP 4.5 projected changes in the probability of occurrence of extreme dry (left) and wet (right) years for the periods 2041-2070 (top) and 2071-2100 (bottom), relative to the baseline period (1971-2004.

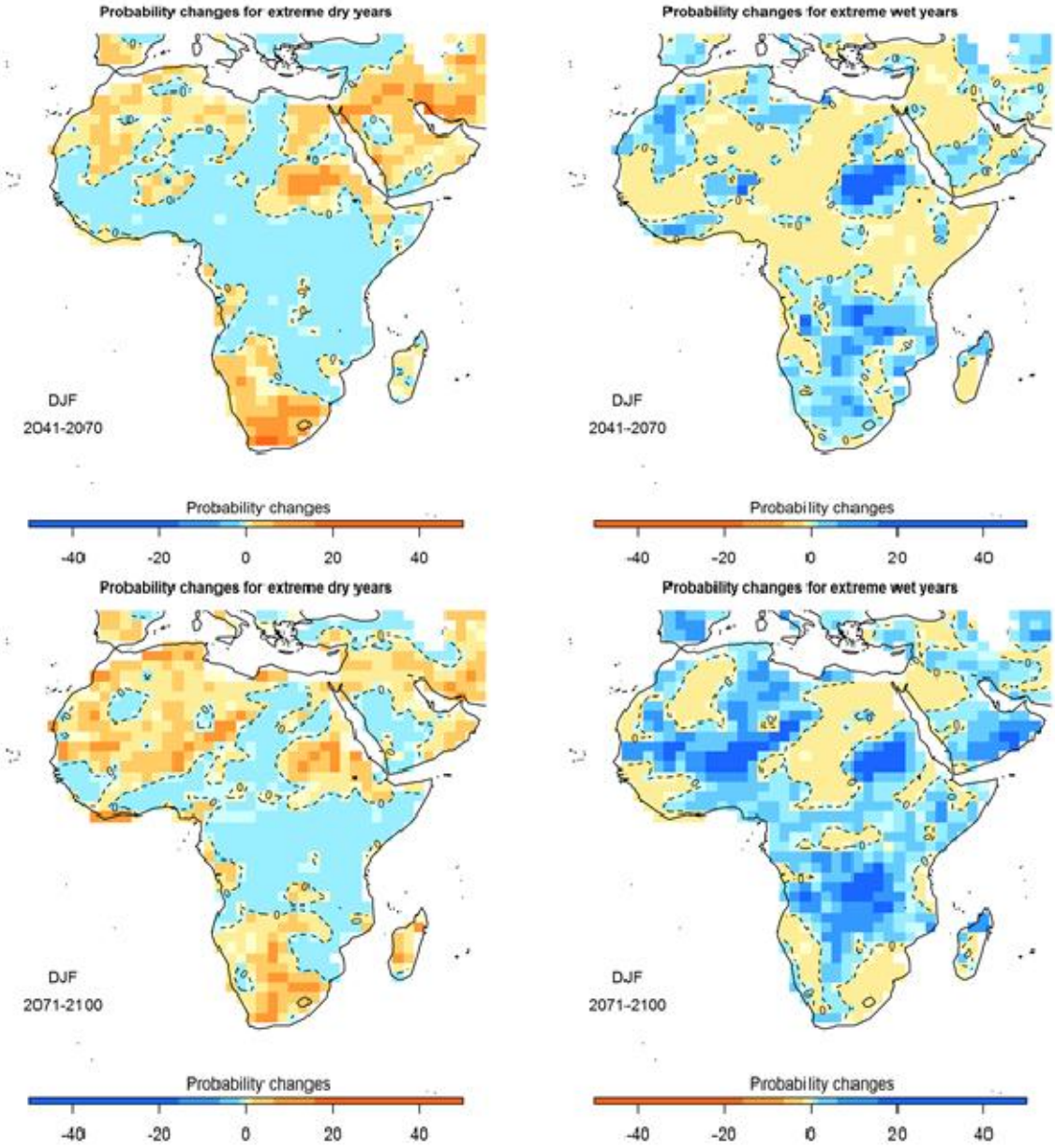

Figure 2.12. CNRM-CM5 RCP 4.5 projected changes in the probability of occurrence of extreme dry (left) and wet (right) DJF seasons for the periods 2041-2070 (top) and 2071-2100 (bottom), relative to the baseline period (1971-2004).

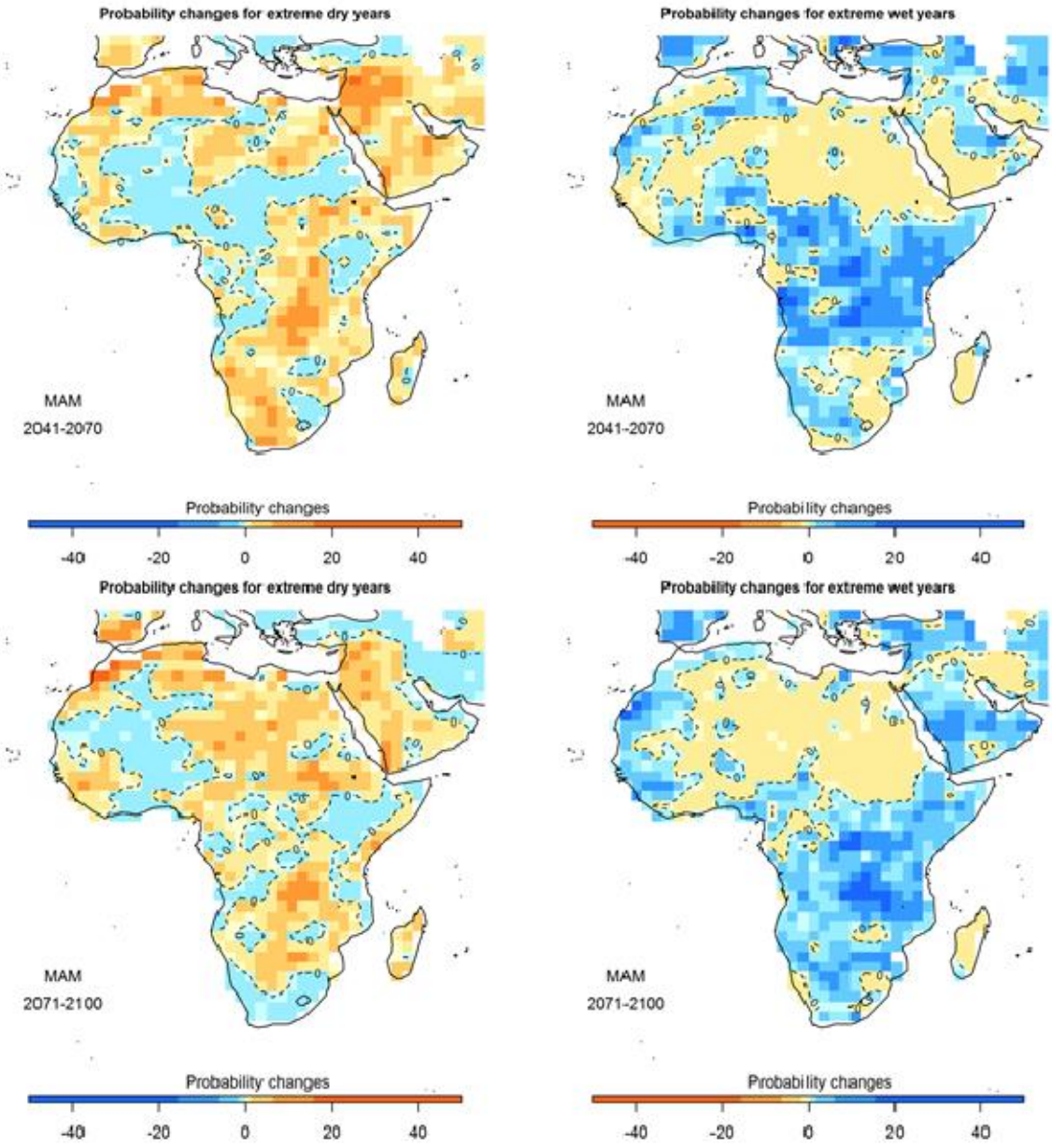

Figure 2.13. CNRM-CM5 RCP 4.5 projected changes in the probability of occurrence of extreme dry (left) and wet (right) MAM seasons for the periods 2041-2070 (top) and 2071-2100 (bottom), relative to the baseline period (1971-2004).

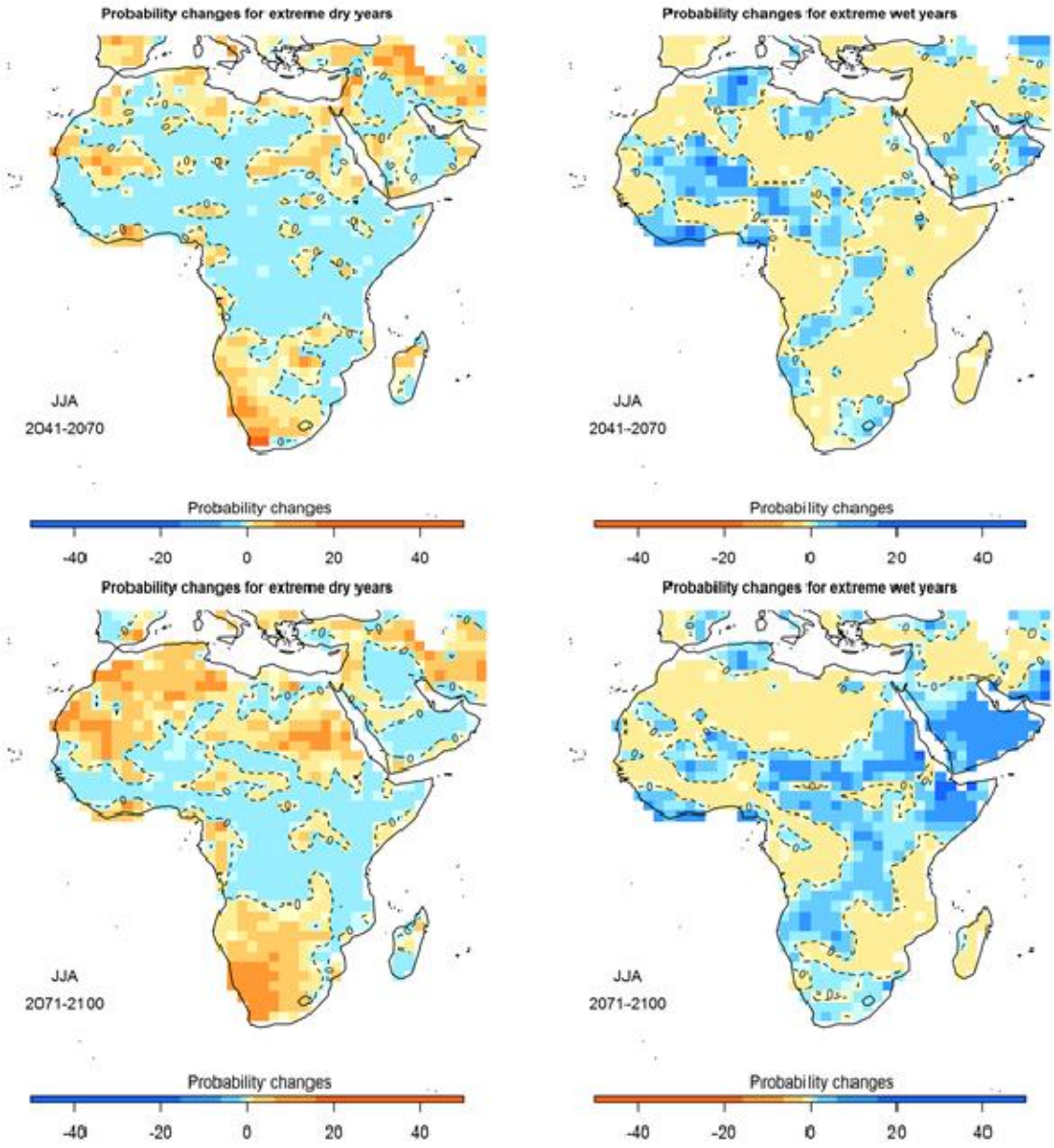

Figure 2.14. CNRM-CM5 RCP 4.5 projected changes in the probability of occurrence of extreme dry (left) and wet (right) JJA seasons for the periods 2041-2070 (top) and 2071-2100 (bottom), relative to the baseline period (1971-2004).

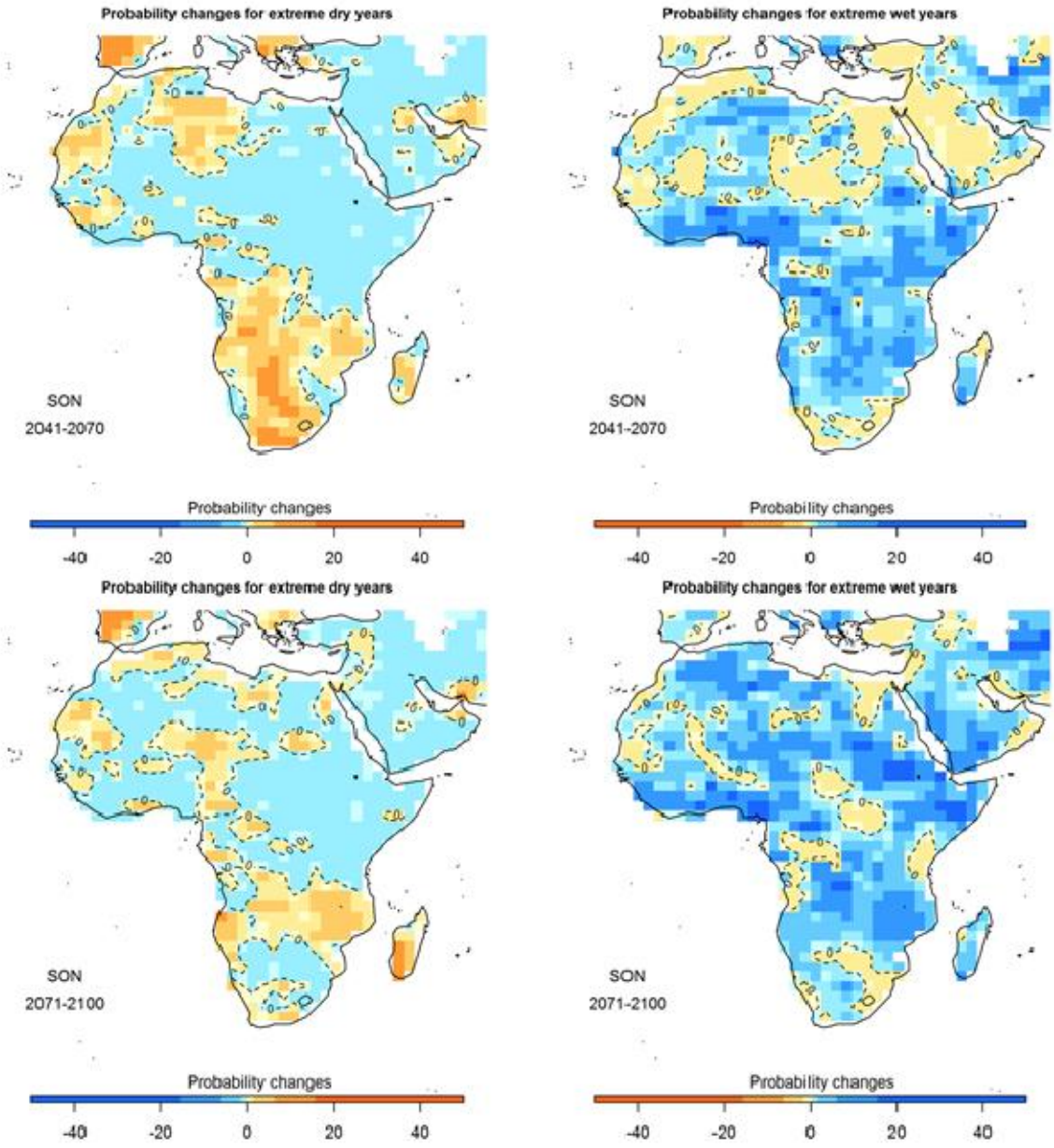

Figure 2.15. CNRM-CM5 RCP 4.5 projected changes in the probability of occurrence of extreme dry (left) and wet (right) SON seasons for the periods 2041-2070 (top) and 2071-2100 (bottom), relative to the baseline period (1971-2004).

Observed variability in drought frequency in Africa

The Global Precipitation Climatology Centre (GPCC) dataset was selected for the analysis of historical drought frequencies over Africa. The GPCC gridded dataset relies only on station data and covers more than a century of data. However, due to possible inhomogenities caused by changes over time in the number and spatial coverage of the stations used, only the period 1959-2010 was used in this report, to compute the SPI baselines.

Having selected SPI as the drought indicator to be used, drought can be defined as a period in which the SPI itself is continuously below a certain threshold (Table 2.1). However, definition of the time scale or aggregation period is required for any specific evaluation since its impacts on different socio-economic systems are dependent on its definition.

Figure 2.16 is a frequency map showing the probability of having SPI below -1 during 1990-2010, for different aggregation periods (3, 6, 9, and 12 months). Here only small differences are observed, mostly in the Sahel where meteorological and agricultural droughts (based on SPI3) are more likely when compared with other aggregation periods. Conversely, in central Africa (e.g. in the Democratic Republic of the Congo) more frequent hydrological droughts are associated with SPI9 and SPI12. Moreover, there exists low frequency oscillations related to drought occurrence and severity. This means that the drought hazard definition is dependent on the aggregation period analysed.

Decadal variability of rainfall over Africa during the 20th century was studied by several authors (Nicholson 1994; Hulme 1996; Moron 1997; Nicholson et al 2000; Nicholson 2001; Kruger 2006; Kane 2009: Malherbe et al., 2012). Relatively dry conditions in the early 20th century prevailed over most of the continent, with exceptions being equatorial East Africa and the areas with a Mediterranean climate. In West Africa relatively wet conditions were observed during the 1920s and 1930s, but relatively dry conditions persisted in much of southern Africa.

The 1940s were characterized by a widespread drought, particularly in West Africa, followed by more extreme fluctuations in the latter half of the 20th century (Nicholson 2001). The 1950s were probably the wettest period since at least the 1870s and 1880s for the whole continent, but a pattern of sub-normal rainfall prevailed in the equatorial regions. In the early 1960s the rainfall increased dramatically throughout most of the equatorial region. By the 1970s, increased dryness was widespread, especially in the early 1970s (Nicholson 1994), but the decade as a whole was relatively wet in much of southern Africa, a result of several years of extremely high rainfall in mid-decade. By the 1980s, rainfall was below the long-term mean over most of Africa, a trend that has continued into the 1990s.

These changes in drought frequencies depicted in Figure 2.16 and Figure 2.17. The well-known dry period that occurred in the middle 1970's in the Sahel and West Africa implies a higher drought frequency over these regions during the period 1970-1989. Another singularity is the low drought frequency over central Africa during the 1970-89 period, followed by a significant increase in drought occurrence during the following 20 years. In that region a hydrological discontinuity (start of a dry period) during the 1970s was detected at almost all the basins in the region (Laraque et al 2001). In particular, for the Congo River at the beginning of the 1980s, a significant drop in the run-off (around 10%) was experienced. This continued until early 2000, with a drop in its inter-annual discharge of 10%. However, for rainfall the change was not as evident, as depicted by Conway et al 2009. The authors didn't find consistent signals in rainfall and river flows across the whole of the region. Central Africa shows very modest decadal variability, with some similarities to the Sahel (dry period starting during mid-1970s). However, care is required in the interpretation of time series and secular variations using global datasets, because some basins have a very low stations density. For instance, at the Congo basin there are a maximum of five gauges across $3.5x10^6$ km^2 (Conway et al., 2009).

2.3.6 Future Changes in Drought duration, frequency and severity

An analysis of the projected changes in the main characteristics of droughts is presented in this section. Droughts were characterized by the duration, frequency and severity of periods, where the SPI is below -1.0.

The results obtained (see Figures 2.19, 2.20 and 2.21) are comparable with results obtained for the probability of occurrence of extreme dry years (Section 2.2.5). In general, the results for all the SPI time scales tend to be in the same direction, but changes are more evident for the higher aggregation periods (i.e., 12 months). In fact, there is a clear signal in the Mediterranean coast of the continent and in most of Southern Africa and Madagascar for drought severity and duration to increase. The largest changes are projected for the northwestern parts of Africa (mainly over Morocco) and over Southern Africa. The increase in drought duration and severity over the North African west coast extends as far south as 15° N. This is consistent with the to the projected systematic poleward shift of storm tracks (e.g. Christensen et al., 2007). These results are valid for both the projected mid- and far-futures. In these regions the projection indicates a slight decrease in drought frequency in the mentioned regions. This is associated with increases in the length and severity of droughts.

On the other hand, most of the inter-tropical regions of the continent exhibit a reduction in all the drought parameters analyzed, under the projected climate futures. Decreases of up to 50% in drought severity and up to 30% in drought duration are projected for central tropical Africa. As discussed previously, these changes may be linked to the expanding tropical belt and increases in tropical convection.

2.3.7 Discussion and conclusions

The CNRM-CM5 RCP 4.5 projection indicates that enhanced anthropogenic forcing may have large effects on drought in the continent, with the largest impacts in the subtropical and mid-latitudinal regions. During all seasons, the probability to have an extreme dry period is projected to increase over the extra-tropics, mainly in the Mediterranean coast and almost the whole of Southern Africa, while such probabilities are projected to decrease over most tropical areas of the continent. Extreme wet seasons are also projected to increase in frequency, except over parts of West Africa and southern South Africa. The magnitude of changes, and specifically the probabilities of occurrences of extreme dry and wet years (and seasons), are generally larger for the far-future than for the mid-future.

Drought severity and duration are projected to increase over the Mediterranean coast and over most of Southern Africa. On the other hand, the tropics are projected to experience decreases in drought duration and frequency.

It should be noted that the CNRM-CM5 RCP 4.5 projection represents a single realization of future climate, and is not sufficient to describe the full uncertainty range of the projected drought futures over Africa. However, the results presented in this section are consistent with those of the DEWFORA CCAM ensemble of projections, with the CGCM projections described in AR4 of the IPCC, and with the main conclusions of a number of additional studies of climate change over Africa (Sheffield and Wood, 2008; Orlowsky and Seneviratne, 2012).

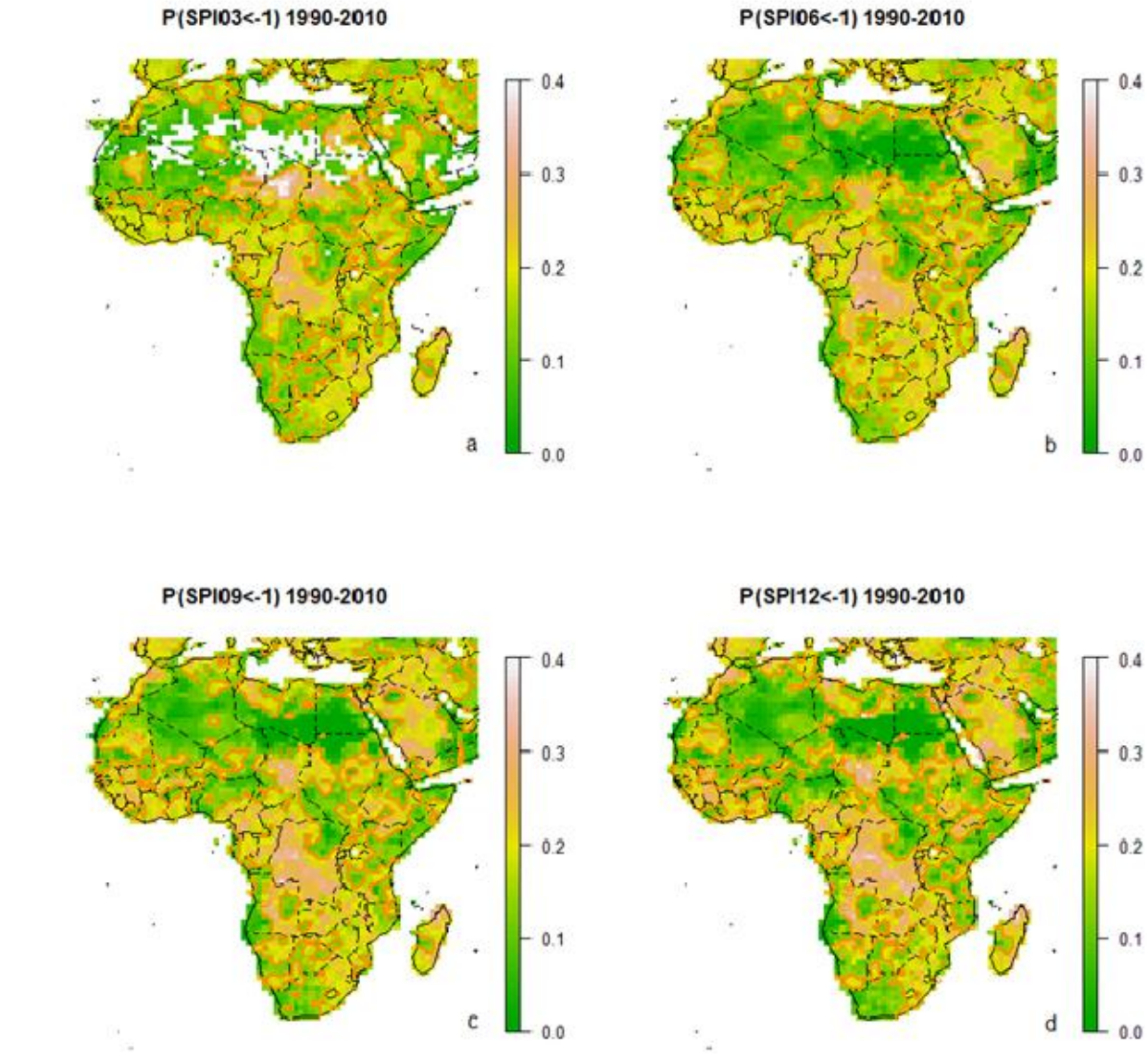

Figure 2.16. Relative frequency of SPI_k < -1 (k: 3, 6, 09, 12 months) during 1990-2010.

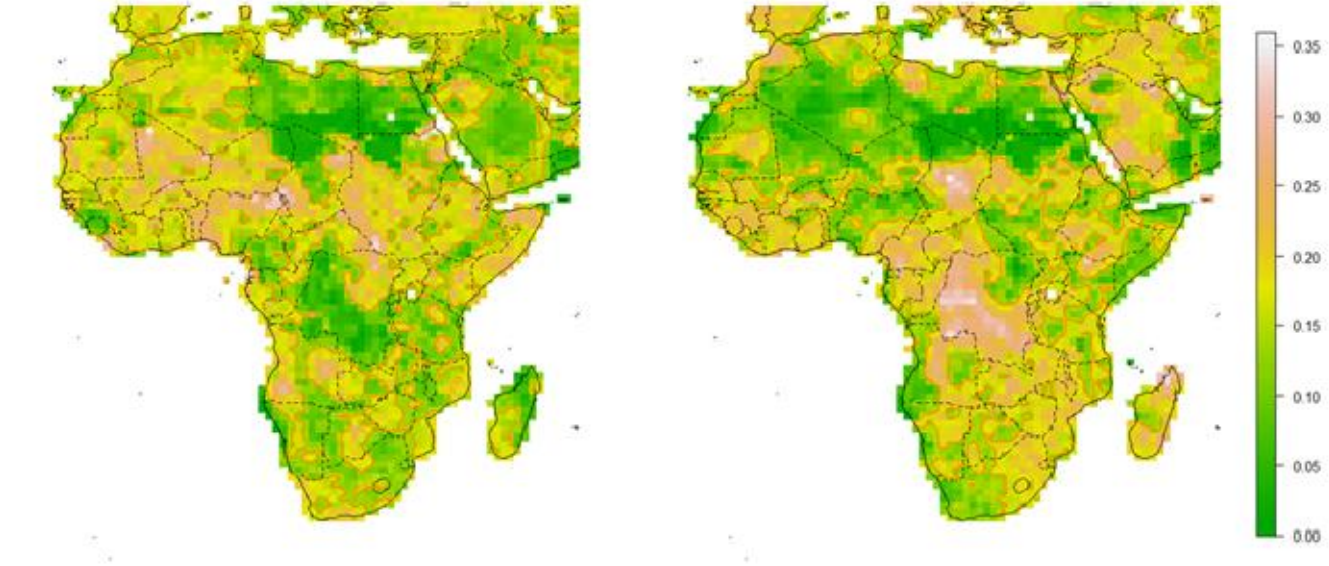

Figure 2.17. Comparison of the relative frequency of SPI06 < -1 for 1970-1989 (left) and 1990-2010 (right).

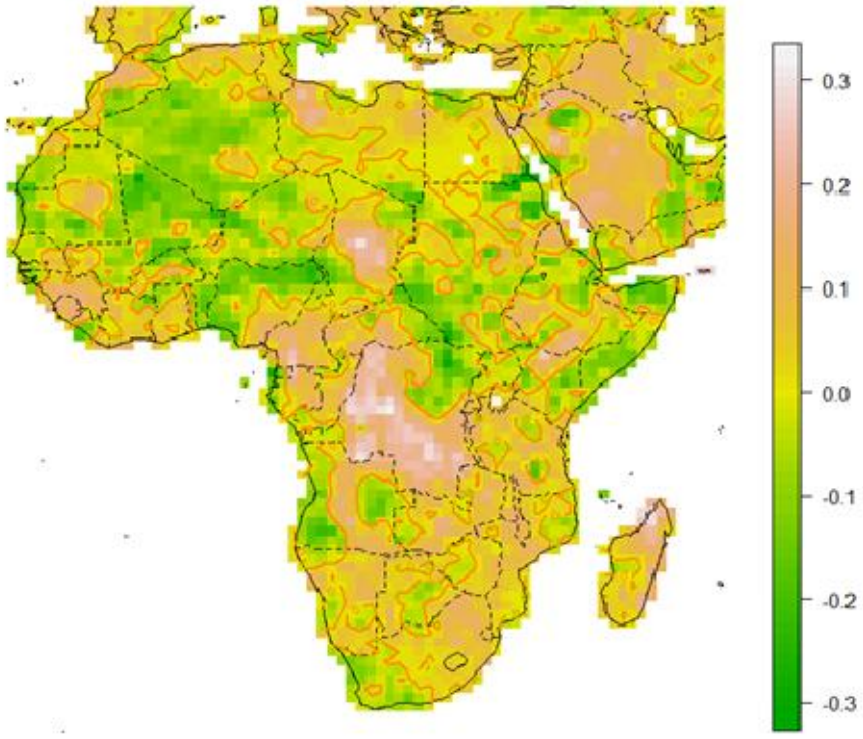

Figure 2.18. Differences between SPI06 <-1 frequencies in 1990-2010 and1970-1990.

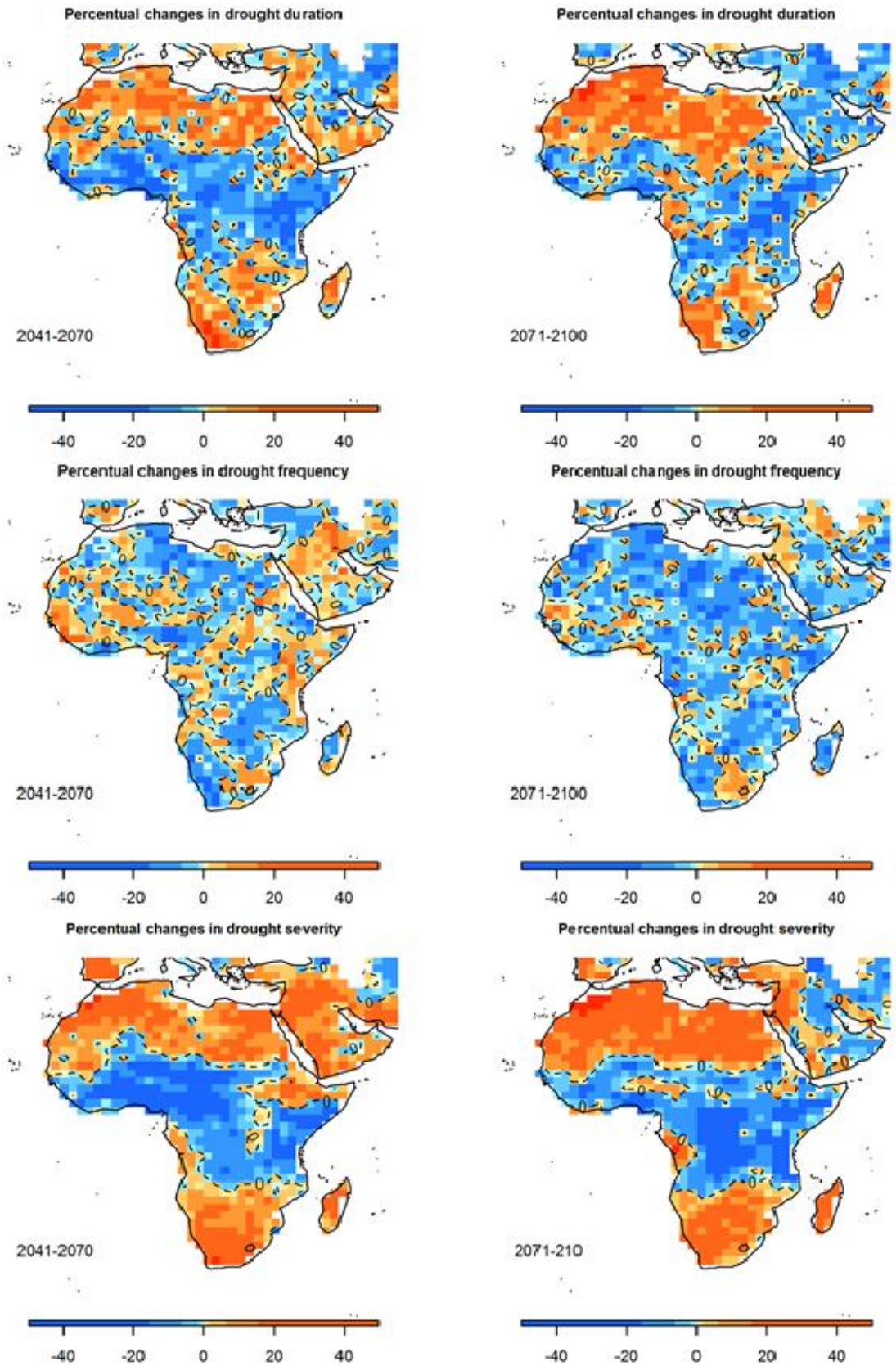

Figure 2.19. Projected changes of drought duration, frequency and severity (expressed as percentage changes) as represented by SPI-01.

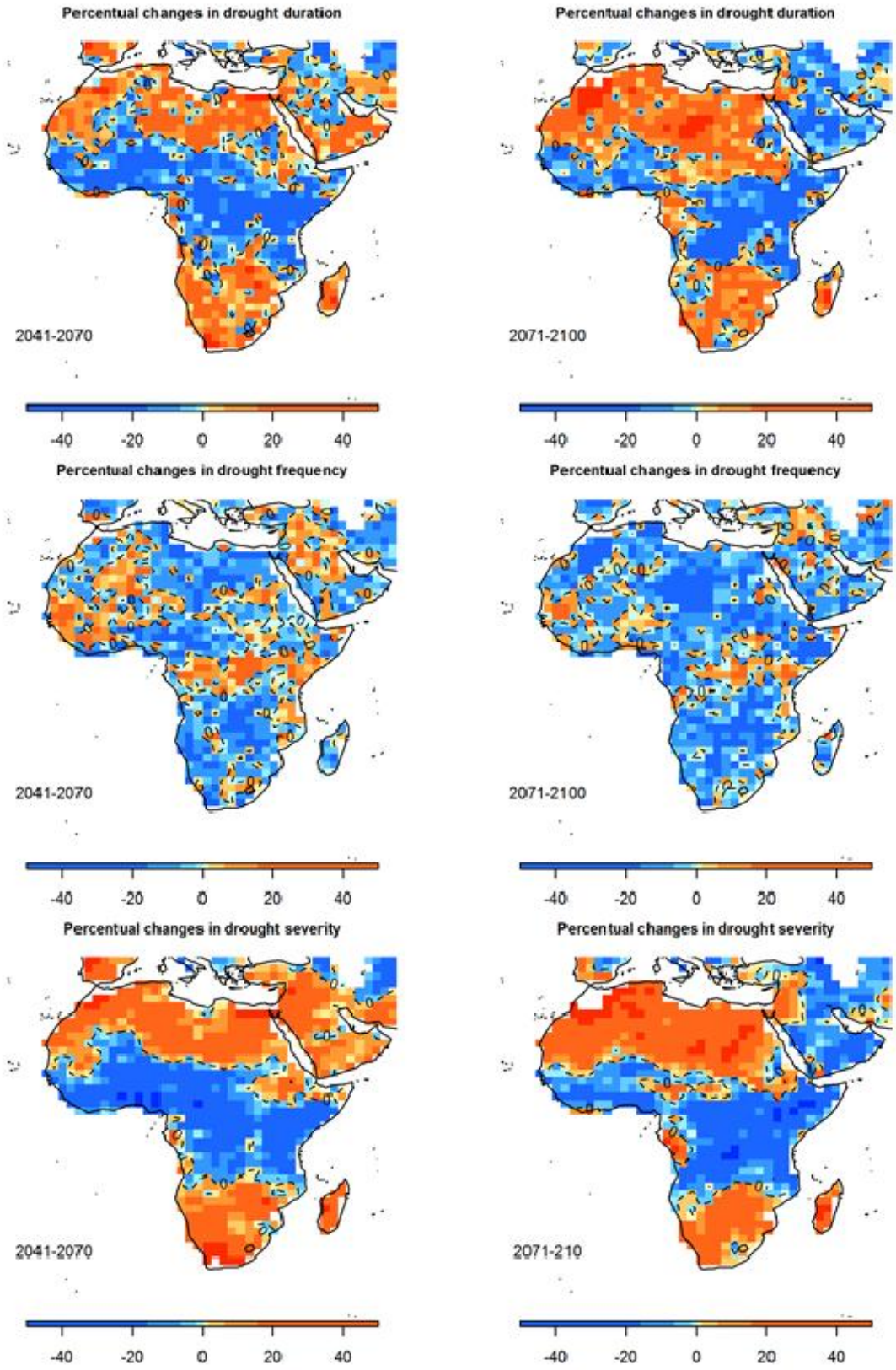

Figure 2.20. Projected changes of drought duration, frequency and severity (expressed as percentage changes) as represented by SPI-03.

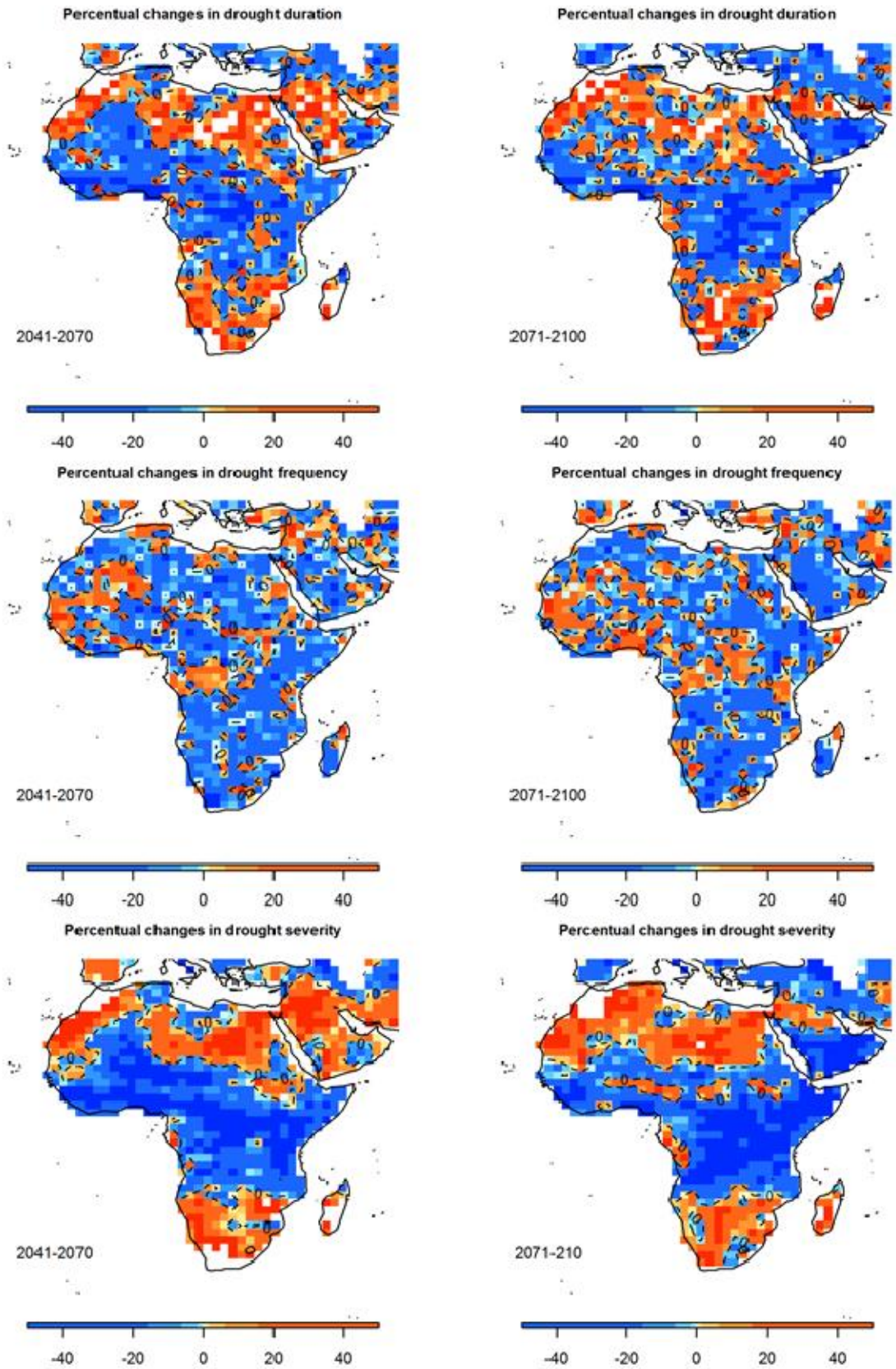

Figure 2.21. Projected changes of drought duration, frequency and severity (expressed as percentage changes) as represented by SPI-12.

3. THE POTENTIAL VALUE OF SEASONAL FORECASTS IN A CHANGING CLIMATE

3.1 INTRODUCTION

The previous sections of this report have illustrated that the African continent is vulnerable to the increased incidence of droughts and the related hazards of heat waves and high fire danger days, under climate change. The skillful forecast of the outbreak of drought over Africa, at the seasonal time-scale, may therefore be regarded as an important adaptation measure to reduce this vulnerability. To further explore this idea, this section of the report explores the projected changes in metrics that are of key importance to the occurrence of drought over Africa. The ability of state-of-the-art present-day seasonal forecasting systems, to skillfully predict the variability of these metrics at inter-annual time-scales, is subsequently explored. The southern African region is the focus area of this component of the report, due to its well-known vulnerability to drought outbreaks during El Niño years, and due to the region having high quality historical records of weather data, which facilitate the verification of seasonal forecasts over the region.

The previous sections of this report have illustrated that the African continent is vulnerable to the increased incidence of droughts and the related hazards of heat waves and high fire danger days, under climate change. The skillful forecast of the outbreak of drought over Africa, at the seasonal time-scale, may therefore be regarded as an important adaptation measure to reduce this vulnerability. In case the frequency of occurrence of such drought events and related hazards will increase in the future, skillful forecast will gain importance. To further explore this idea, this section of the report investigates the projected changes in metrics that are of key importance to subsistence farmers (rainfed agriculture and dairy farming). These groups experience impacts of droughts during successive dry days (rainfed farming) and heat waves (dairy farming). The focus is therefore on projected changes in frequency of these metrics. The ability of state-of-the-art present-day seasonal forecasting systems, to skillfully predict the variability of these metrics at inter-annual time-scales, is subsequently explored. The southern African region is the focus area of this component of the report, due to its well-known vulnerability to drought outbreaks during El Niño years, and due to the region having high quality historical records of weather data, which facilitate the verification of seasonal forecasts over the region[1].

Southern Africa is largely a semi-arid region, experiencing substantial inter- and intra-annual climate variability (Barron et al., 2003; Nyakudya and Stroosnijder, 2011). This variability expresses itself both in rainfall and temperature and frequently causes negative impacts on agricultural activities, which are often of a smallholder nature and reliant on limited resources. Throughout Sub-Saharan Africa, 95% of cultivated land is under rain-fed agriculture (Parr et al., 1990; Rockström, 2003). Given the limited extent and scope for development of surface water irrigation, most countries in Southern African rely strongly on rain-fed agriculture. Therefore, precipitation patterns, timings and amounts are directly correlated to crop yield and indirectly to food security and resilience to climate variability. While a lower total amount of rainfall over the crop growing season will influence the crop yield, it is often the poor distribution of rainfall resulting in dry-spells and wet-spells that is the cause for reduced crop yields (Barron and Okwach, 2005; Ingram et al., 2002; Ochola and Kerkides, 2003; Rockström, 2000). In particular, maize (Zea mays L.) is sensitive to the occurrence of dry spells as well as insufficient rain for seedlings (due to too early planting) (see e.g. Barron et al., 2003; Nyakudya and Stroosnijder, 2011). Given the typical length of

[1] The contents of this chapter were adapted from Winsemius et al. (2013). Full reference: Winsemius, H. C., Dutra, E., Engelbrecht, F. A., Archer Van Garderen, E., Wetterhall, F., Pappenberger, F. and Werner, M. G. F.: The potential value of seasonal forecasts in a changing climate, Hydrol. Earth Syst. Sci. Discuss., 10(12), 14747–14782, doi:10.5194/hessd-10-14747-2013, 2013.

the growing season for maize (120-140 days) and the relatively short rainy season across large parts of Southern Africa, maize is considered a particularly vulnerable crop if it is grown on rain-fed farms. Dairy and other livestock farming may further suffer seriously from climate change (Archer van Garderen, 2011, Nesamvuni et al, 2012). Dairy production remains fairly stable under a range of climate conditions, but reduces significantly up to 20% with increasing heat stress above a threshold (Ravagnolo et al., 2000). Heat stress is caused by the combined effects of dry bulb temperature, humidity, solar radiation and wind speed (Dikmen and Hansen, 2009). When a hot period ends, the productivity does not necessary return to normal values immediately (Ravagnolo et al., 2000). The drop in productivity is generally proportional to the length of the hot period.

Current variability in climate may already cause substantial reductions in agricultural yields. There is concern that climate change may aggravate the effects of this variability, due to decreasing or more erratic rainfall, as well as an overall increase in temperature leading to more frequent occurrence of livestock heat stress conditions (Archer van Garderen, 2011; Davis, n.d.; Hetem et al., 2011; Kusangaya et al., in revision; Nardone et al., 2010; Nesamvuni et al., 2012; Ziervogel et al., in revision). These changes may make the agricultural sector throughout Southern Africa vulnerable. As a consequence, the importance of forecasting, warning and strengthening of preparedness (see e.g. Carsell et al., 2004) to mitigate the effects of negatively impacting climate variability may increase. This requires: (1) adequate skill of such forecasts to detect critical weather conditions for the agricultural sector; and (2) that sufficient mitigation measures for response are in place. Reducing the impact of dry spells on the yield may be achieved through local mitigation measures such as rainwater harvesting techniques (Brown and Hansen, 2008), or temporary supplementary irrigation from for example on-farm ponds (Barron and Okwach, 2005). Predictions of dry spells across the growing season and in particular during the periods most sensitive to the impact of dry spells help to plan such mitigation measures and optimize the use of a scarce commodity such as water stored in on-farm ponds. Prediction of heat stress conditions aids farmers in deciding upon the planning of anti-heat stress measures such as additional water points, sprinkling, reduced handling (e.g. transportation or moving camps), setting up of shaded areas, as well as specialized attention to vulnerable herd groups (Ravagnolo et al., 2000).

The importance of predictability of indicators, which are tailored to specific end-users such as rain-fed agriculture, is acknowledged by Reason et al. (2005). They investigated the inter-annual variability of dry spells within the rainy season and anomalies in the onset of rainy seasons over the Limpopo basin. Reason et al. (2005) found significant relationship between these indicators and Nino 3.4 sea surface temperature (SST). They suggest that within the Limpopo region, predictability of the rainfall characteristics at the seasonal scale may exist. In fact, Landman and Beraki (2012) have demonstrated that seasonal forecasts of mid-summer rainfall totals over the Limpopo region are skillful during years of strong ENSO forcing. In addition ambient temperature, required to estimate potential heat stress, shows seasonal predictability in the Southern African region using SST according to Barnston and Smith (1996). Particularly during the rainy season, the predictability is very high, and is not even very strongly dependent on lead time. However, seasonal predictions need to be transformed into meaningful indicators for end-users, to be useful to inform decisions in planning cropping patterns, planting period, and heat stress relieving measures.

In this paper we investigate whether weather conditions critical for subsistence farming in Southern Africa, are likely to increase in a changing climate, and if so, whether current seasonal forecasts are good enough to detect these skilfully. If this is the case, then the importance of seasonal forecasts may be expected to increase in the future because planning of timely mitigation actions will be needed more frequently. Critical weather conditions are expressed as indicators with defined thresholds that are meaningful for end-user decision making. We apply here two indicators: (1) frequency of dry spells of a defined minimum length and (2) frequency of days with heat stress conditions expressed in the Temperature Heat Index (THI) above a defined threshold. First this paper describes whether the frequency of these critical conditions are projected to change under enhanced

anthropogenic forcing, according to Regional Climate Model (RCM) simulations. In addition the skill of seasonal forecasts in reproducing the inter-annual variability in the frequency of the indicators and thresholds across the rainy season is quantified. In section 4.2 we outline the methodology, Section 4.3 describes the results of the study, which are further discussed in light of the importance of forecasts in a changing climate in section 4.4. In this section, we also discuss limitations of the research. Conclusions on the changing potential of seasonal forecasts over southern Africa in a changing climate are provided in section 5.

3.2 METHODOLOGY

3.2.1 Area and time-period of study

This component of the report focuses on Southern Africa (Latitudes -35˚ to -10˚, Longitude from 10˚ to 55˚), and in particular the Limpopo river basin. The Limpopo Basin is shared by four countries; namely Botswana, South Africa, Zimbabwe and Mozambique. It is an area widely acknowledged to have critically stressed access to water (LIMCOM, 2010). While data availability and compatibility between the four countries to produce basin estimates remains a challenge (LIMCOM, 2010), regular food security and vulnerability estimates are made by the Regional Vulnerability Assessment Committee (RVAC). They provide cereal production and livestock production outlooks for the four basin member countries, as part of the Southern African Development Community (SADC). For example, for the 2011/12 season, the cereal surplus/deficit was indicated as -356 ('000 tons), -856, -3522, and -834 for Botswana, Mozambique, South Africa and Zimbabwe respectively (RVAC, 2011); while livestock production for beef for the whole of mainland SADC from 2006 through 2010 increased from 1.25 to 1.45 million tons (RVAC, 2011).

The rainy season and therefore also the cropping season in the Limpopo concentrates in the months December, January and February (DJF). The precipitation is highly variable in terms of total amount, onset and intermittency (Engelbrecht et al., 2013; Kane, 2009; Love et al., 2010; Reason et al., 2005; Usman and Reason, 2004). DJF is also the season with the highest temperatures and therefore the highest probability of livestock heat stress conditions. We therefore focus our analysis on the DJF season.

3.2.2 Data used

Seasonal forecasts

Seasonal forecasts provide information on the development of the climate up to 6 to 12 months ahead, rather than detailed day-by-day variations. Probabilistic seasonal forecast systems have significantly more skill than deterministic forecasts (Molteni et al., 2011), and such probabilistic information can be used by end-users in support of decision-making (see O'brien, 2002; Ramos et al., 2013, 2010). In this study we use the ECMWF System 4 seasonal forecast system (S4, Molteni et al., 2011), based on an atmosphere-ocean coupled model, which has been operational since November 2011. The atmospheric model has a horizontal resolution of about 79 km with 91 vertical levels and the ocean model has a horizontal resolution of approximately 1° with 42 vertical levels. The seasonal forecasts consist of a 51-member ensemble with 7-months lead time, including the month of issue, referred as 0-month lead time. S4 has a set of re-forecasts (or hindcasts) starting on the first of every month for the period January 1981 to December 2010. The hindcast set is provided for calibration purposes with the same configuration as the operational forecasts, except in the ensemble size: 51 members for the initial forecast dates of February, May, August, and November; and 15 members for the remaining initial forecast dates. Molteni et al. (2011) presents an overview of S4 model biases and forecast performance. Dutra et al. (2013) and Mwangi et al (submitted) evaluated the S4 in terms of meteorological droughts in several African Basins and areas. Mwangi et al. (submitted) conclude that ECMWF seasonal forecasts add value to the statistical forecasts currently in operations at the Horn of Africa.

ERA Interim reanalysis

The ECMWF reanalysis ERA-Interim (ERAI, Dee et al., 2011), available since 1979 to present, was used in this study to verify the skill of the seasonal forecasts. The atmospheric model has the same resolution as the seasonal forecasts (about 79km) and is associated with a 4D-var data assimilation scheme for the optimal consistency between globally available observations and model background. 2-meter temperature and dew point temperature (used in this study to derive relative humidity) are analysed over land separately from the main atmospheric analysis. An optimal interpolation scheme produces 6-hourly estimates of 2-meter temperature and dew point temperature combining synoptic observations with background estimates derived from the latest atmospheric analysis. Therefore, over densely observed areas, ERAI 2-meter temperature and dew point temperature can be considered close to observations. On the other hand, precipitation is a forecast product generated by the atmospheric model. This can lead to significant biases in ERAI precipitation (from daily to inter-annual scales). Dutra et al. (2013) show that over South Africa, and in particular the Limpopo basin, ERAI monthly precipitation has good agreement with observations in terms of intensity and inter-annual variability. On the daily time-scales, Belo-Pereira et al. (2011) found a reasonable performance of ERAI over the Iberian Peninsula despite an overestimation of wet days (excessive drizzle).

Bias corrected Cubic Conformal Atmospheric Model simulations

An ensemble of regional projections of future climate change over southern Africa, obtained using the conformal-cubic atmospheric model (CCAM), are examined in this section. CCAM is a variable-resolution global atmospheric model, developed by the Commonwealth Scientific and Industrial Research Organisation (CSIRO) in Australia (McGregor and Dix, 2008; McGregor, 2005). When applied in stretched-grid mode, the model provides a flexible and computationally efficient way of downscaling coupled global climate model (CGCM) projections to high resolution over an area of interest. The projections described here were obtained by downscaling the simulations of six CGCM projections reported in Assessment Report Four (AR4) and the Coupled Model Intercomparison Project Phase 3 (CMIP3) to high resolution over southern and tropical Africa. All six CGCM projections are for the period 1961-2100, and for the A2 emission scenario of the Special Report on Emission Scenarios (SRES). The bias-corrected sea-surface temperatures (SSTs) and sea-ice concentrations of the CGCM projections were first used to force CCAM simulations at a quasi-uniform horizontal resolution of about 200 km. These simulations were subsequently applied for the nudging of high resolution (about 60 km) simulations over southern and tropical Africa. Detailed descriptions of the CGCMs used can be found in Malherbe et al. (2013). The CCAM downscaling procedure over Africa is described in more detail by Engelbrecht et al. (2011). The model's ability to simulate the present-day characteristics of regional climate has earlier been investigated rigorously over southern Africa (e.g. Engelbrecht et al., 2013, 2009; Landman et al., 2009) and for various other climatological regions (e.g. Lal et al., 2008; Nunez and McGregor, 2007).

To reduce systematic differences between present-day climate and model simulated present-day climate, a simple monthly-scale mean bias-correction procedure was applied in this research, using the CRU TS3.1 data set of the Climatic Research Unit (CRU, Mitchell and Jones, 2005) as reference climate. Precipitation has been corrected with a multiplicative correction factor, while all other variables have been corrected with an additive correction.

3.2.3 Selection and definition of indicators and thresholds

Both the seasonal forecasts as well as the projections of future climate change are analysed in terms of the frequency of occurrence of certain critical thresholds being exceeded. Each critical condition is expressed in an indicator, along with a threshold that measures the intensity of the event. Both indicators and thresholds are selected so that they are meaningful for end users, and cover the two most important agricultural activities in the basin:

- Dry spells: rain-fed agriculture is particularly vulnerable for dry spells within the growing season. While a lower total amount of rainfall during the crop growing season will influence the yield, it is more often the erratic temporal distribution of rainfall resulting in dry and wet spells that is the cause for reduced crop yields or even failure (Barron et al., 2003; Ochola and Kerkides, 2003; Usman and Reason, 2004). Both the frequency of occurrence of such dry spells and their length are important. We compute a dry spell by treating the rainfall time series as a Markov process (see e.g. Barron et al., 2003; De Groen and Savenije, 2006) where a dry day is given when rainfall is below 1 mm per day. It is assumed that 1 mm per day evaporates as interception or bare soil evaporation and does not take part in the plant production process (Gerrits et al., 2007; De Groen and Savenije, 2006; Savenije, 2004). As thresholds, dry period durations of 3, 5 and 10 days were selected, which are in the order of the length, potentially causing reduced crop productivity. Since the indicator is of a non-continuous nature (i.e. a number of days), the amount of possible values for the frequency of spells in a given period of time, reduces significantly with the threshold chosen (i.e. the theoretical maximum frequency of occurrence of a 15 day dry spell within one month is by default 2). Therefore the estimation of the climatology of the frequency of occurrence of dry spells longer than 10 days is compromised by the fact that too few unique values can be expected within the distribution. Dry periods longer than 10 days are therefore not considered for analysis here.

- Temperature Heat Index (THI): THI is an empirical, unit-less measure and is a function of temperature and air humidity. The THI can be used as a measure for livestock heat stress, resulting in a serious decline in milk production / water use ratios. In this paper, THI is computed following the formulation of Dikmen and Hansen (2009):

$$I_{TH} = (c_1 T + c_2) - c_3 (1 - H)(c_1 T - c_4),$$

where I_{TH} is the THI [-], T is the ambient temperature [˚C], H is the ambient relative humidity [-] and c_1 to c_4 are empirically derived constants with the respective values 1.8 ˚C^{-1}, 32, 0.55 ˚C^{-1} and 26.8. As thresholds, we selected a THI of 72 as an indicator for mild stress, and 78 as an indicator of severe stress (Nesamvuni et al., 2012; Ravagnolo et al., 2000). We applied Eq. 1.1 using the maximum ambient temperature on each day.

3.2.4 Data analysis

In order to estimate trends in changes in the frequency of occurrence of the chosen indicator and threshold combinations, climatologies for different indicator/threshold combinations over the full DJF season were established. These climatologies were derived over the following 40-year periods: 1961-2000, 2011-2050, 2061-2100. The following procedure was followed to obtain the climatologies:

- First daily time series were established for each of the two indicators over the period of interest (e.g. 1961-2000), using precipitation for a Markov-based dry spell length estimation, and temperature and relative humidity for the estimation of THI.
- Counts of the amounts of occurrences of each indicator / threshold combination were subsequently performed, for the DJF season and for each of the periods of interest. This yielded 40 values at each grid cell in the domain of interest - one value for each year of the period of interest.
- Based on the 40 values, a climatological distribution of the indicator / threshold combination was established. The distribution may be expressed in the form of selected quantiles. Because the amount of samples (40) is limited, samples of the 8 neighbouring cells of each cell under consideration were also included to develop the

climatological distribution. This resulted in a sample size of 40 × 9 = 360 samples per cell.

It was subsequently investigated whether the climatology of the DJF indicator / threshold combinations shows a significant increase in the frequency of occurrence, compared to the natural variability. If this is indeed the case, it would imply a growing importance to have skilful seasonal forecasts.

The skill of the ECMWF S4 seasonal forecasts was assessed over the hindcast period (1981-2010) taking ERAI as verification, and following the same methodology for the indicators/threshold calculations as described before for the climate simulations. Three different scores were used to assess skill: correlation, relative operating characteristics (ROC) and reliability (REL) diagrams. The correlation is a deterministic score (only considering the ensemble mean), while ROC and REL evaluate probabilistic categorical forecasts. The scores uncertainties due to temporal sampling were assessed by performing 1000 bootstrap samples.

3.3 RESULTS

In the following two sections the effect of climate change on dry spell and heat stress frequency is presented along with the skill of the current seasonal forecasts in predicting these conditions.

3.3.1 Effect of climate change on dry spell and heat stress frequency

To demonstrate how climate change affects the chosen indicator/threshold combinations, we show the 30^{th} and 70^{th} percentiles of the distribution of the chosen indicator/threshold combinations. Figure 3.1 shows the changes in the distribution of the DJF frequency of occurrence of dry spells longer than 5 days over the time slices 1961-2000, 2011-2050 and 2061-2100, for all 6 climate projections. The 5-day threshold is shown, because of the issue with reducing amounts of unique values for frequency of occurrence of dry spells with long durations. The percentile values do not change significantly over the different time slices, and are clearly smaller than the current climate variability (Figure 3.1 panels a-d). We can therefore not conclude from the RCM projections that the frequency of dry spells will increase in the future.

In Figure 3.2, the changes in distribution of the DJF frequency of days with THI higher than 78 are given. The variability in the current climate is not very large, but the climate scenarios project a considerable change by the end of the century. In fact, as mentioned earlier, dairy cattle stress is known to be severe with THI > 78 (Nesamvuni et al., 2012; Ravagnolo et al., 2000) and according to these results, such conditions are largely restricted to the lower valleys as well as the Kalahari desert under present-day climate, but are likely to increase drastically in frequency towards 2100 across most countries north of South Africa (including the northern parts of South Africa itself). Similar increases are projected to occur in the frequency of occurrence of THI larger than 72 and 84 (not shown). According to these results, THI above 84 is rarely occurs in the studied region under present-day climate, but is projected to occur quite frequently in the future over the Kalahari Desert, as well as the lower Zambezi basin. THI exceedances of this type would stress most livestock, which is clearly a significant concern for these areas.

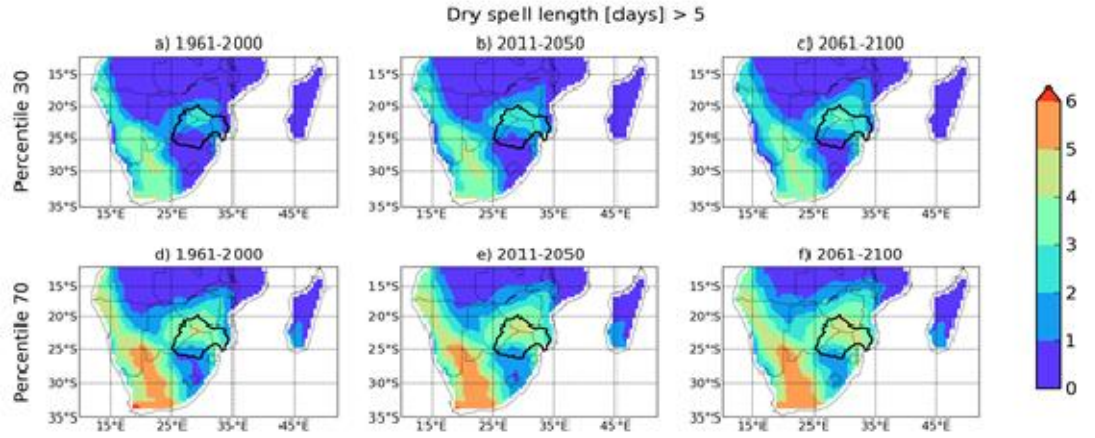

Figure 3.1. Changes in the climatology of DJF frequency of occurrence of dry spells longer than 5 days. The top row (a-c) shows the 30 percentile. The bottom (d-f) shows the 70 percentile. From left to right, the changes in dry-spell frequency climatology are shown along different time slices in the RCM runs (1961-2000, 2011-2050 and 2061-2100).

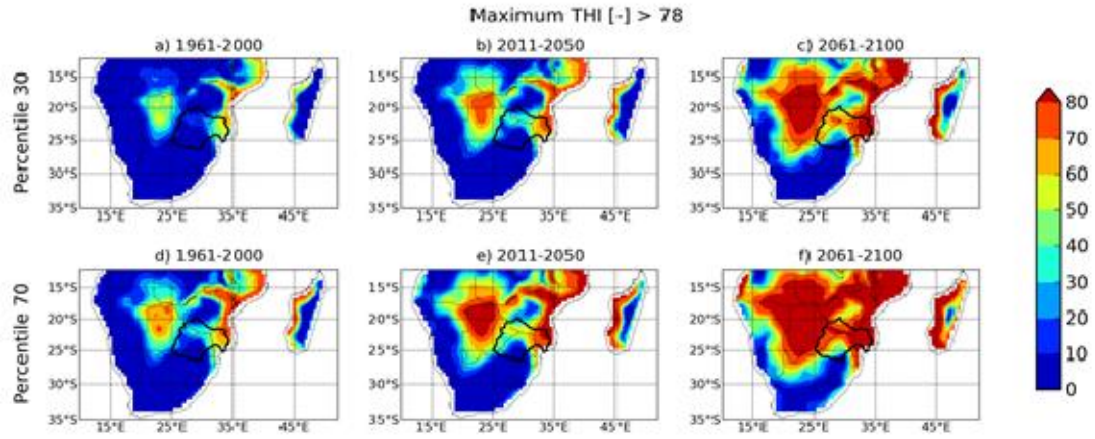

Figure 3.2. Same as Figure 3.1 but for changes in the climatology of DJF frequency of occurrence of days with THI higher than 78.

Figure 3.3 shows the spatial average of the changes in distributions of both the DJF 5-day dry spell frequency (a) and the frequency of THI above 78 (b), averaged over the Limpopo basin. The six individual RCM projections indicate only a very small increase (in particular compared to the current climate variability) in the amount of dry spells, from now until the end of the 21st century. THI above 78 indicates a clear increase in frequency, far larger than the natural climate variability. The individual climate runs are also quite consistent, showing a relatively small variability in the projected change amongst the climate runs. In fact, this result demonstrates that if the IPCC A2 scenario becomes reality, on average an increase of a factor 3 to 4 of the number of days with severe heat stress in the DJF season is to be expected, leading to a total of about 60 days of heat stress during below normal conditions (percentile 30) and about 70 during above normal conditions (percentile 70). This accounts for about 70% of all days within the DJF season compared to about 20% (20 days) in the current climate. These results can also be confirmed for the other THI thresholds (not shown).

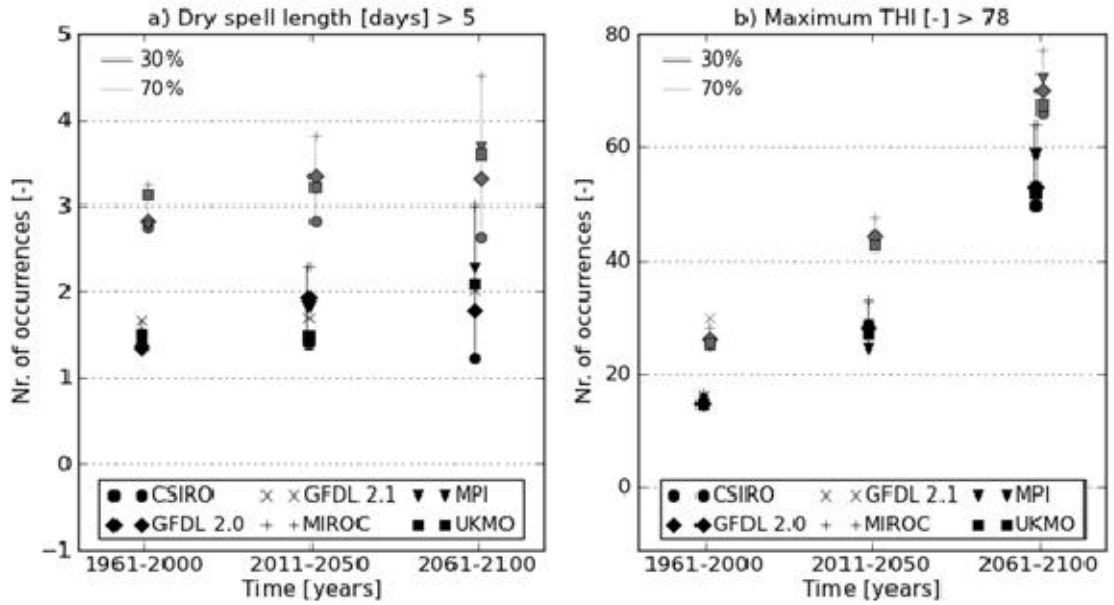

Figure 3.3. Limpopo basin-averaged changes in climatology from 1961-2000 to 2011-2050 to 2061-2100, of DJF frequency of occurrence of dry spells longer than 5 days according to the 6 RCM projections. The dark symbols denote the 30 percentile. The grey symbols denote the 70 percentile. The dark lines indicate the multi-model range for the 30 percentile. The grey lines indicate the multi-model range for the 70 percentile.

3.3.2 Seasonal forecast of dry spell and heat stress frequency

Climatology of the indicator-threshold combinations

Following a similar approach to the climate change analysis, the DJF 30 and 70 percentiles climatology of the frequency of dry spells of at least 5 days and number of days with THI above 78 were compared for different S4 forecast initial dates and ERAI over the period 1981-2010. There is a reasonable agreement (in terms of spatial patterns and intensity) between S4 and ERAI climatologies of the frequency of dry spells of at least 5 days (Figure 3.5). For the number of days with THI above 78, the S4 climatology displays a pronounced underestimation when compared with ERAI and a “cold” drift (lower THI) with lead time (panels a),b),c) compared with d) and panels e), f), g) compared with h) in Figure 3.6). This drift is likely to be associated with changes in sea surface temperature with lead time in the coupled atmosphere-ocean model. This confirms that the forecasts should be disseminated as anomalies, rather than absolute values. The skill assessment is therefore also set up in this way. The comparison between S4 and ERAI mean frequency of the indicators over the Limpopo basin in Figure 3.7 further supports these results.

The year-to-year variability of the climate simulations for the current climate cannot be directly compared with ERAI or S4. However, the time series of the Limpopo averages in Figure 3.7 show similar mean values and inter annual variability between the RCMs and ERAI and S4. In fact, the RCMs do not exhibit the “cold” bias in THI as seen in S4 (Figure 3.7b), due to the bias correction applied to the climate simulations output (see section 2.2). Figure 3.7 also displays the projected time evolution of the indicators for the period 2079-2100. There is a considerable increase in the number of days with THI above 78 while there is no clear difference in the frequency of dry spells of at least 5 days. Similar results were found for the frequency of dry spells of at least 3 days and number of days with THI above 72 (not shown).

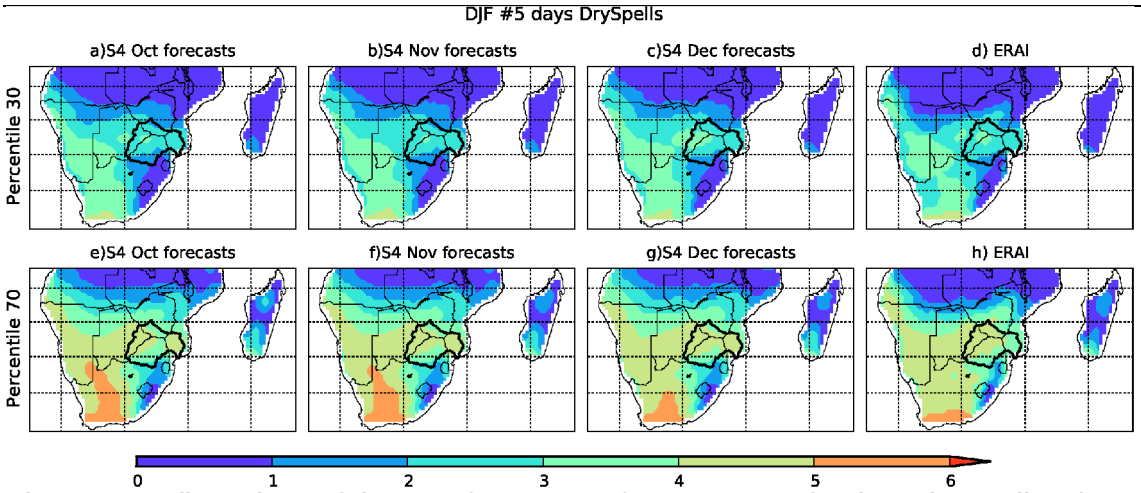

Figure 3.5. Climatology of the DJF frequency of occurrence of 5 days dry spells. The top row (a-d) shows the 30 percentile and the bottom row (e-h) the 70 percentile. From left to right ECMWF S4 forecasts initialized in October (a, e), November (b, f) and December (c, g) and from ERA-Interim (d, h).

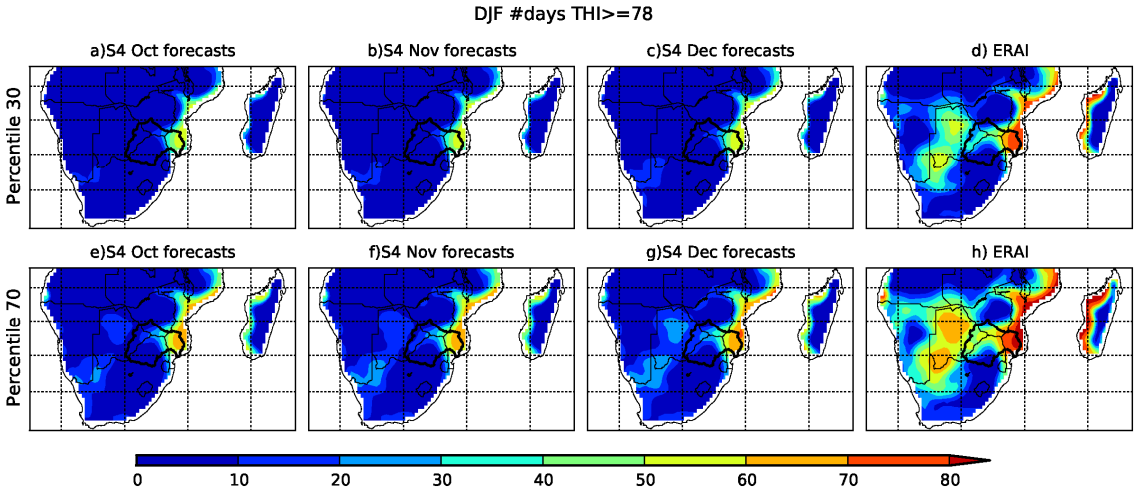

Figure 3.6. Same as Figure 3.5 but the climatology of DJF frequency of occurrence of days with THI higher than 78.

Forecast skill

Grid by grid point correlations (not shown here) indicate that a large fraction of the Limpopo region exhibits significant correlations for all indicators, in particular for the December and November initial forecast dates (i.e. forecasts closest to the DJF season). In detail, the THI forecasts show a much higher correlation than the dry spell forecasts. Nevertheless, also the dry spell forecasts reveal correlation, in particular over the Limpopo and north of the Limpopo (lower Zambezi).

A more detailed analysis of forecast skill was performed over the Limpopo basin. Figure 3.8 shows the mean of the grid-point correlation as well as Relative Operating Characteristic (ROC) scores for above-normal conditions over the Limpopo for each lead time. The 70 percentile is used as threshold to indicate above-normal conditions. Above-normal conditions in this context means a higher frequency of stress conditions, so is therefore of most interest to predict with skill .The figures also show the impact of having 15 ensemble members, with respect to 51 ensemble members (dark versus gray lines). This impact is relatively small although with 51 members, the scores are slightly higher. All ROC scores, including normal (between 30 and 70 percentile) and below-normal (below 30 percentile) conditions are also given in Table 3.1 (dry spells) and Table 3. 2 (THI). The scores show that both indicators have skill (ROC above 0.5). In particular above-normal conditions of the frequency of days

with THI above 78 can be forecast remarkably well by the S4 forecasts. Table 3.1 and Table 3. 2 also show that it is easier to skilfully predict above-normal and below-normal conditions than normal conditions. These findings are consistent with those of Landman et al. (2012), who found that there is skill in predicting inter-annual variability in summer rainfall totals over southern Africa for the below- and above-normal categories, but that forecasts for the near-normal category have little skill. The ROC scores for normal conditions are clearly lower, sometimes even showing no skill at all (ROC score of 0.5) while above-normal and below-normal can be predicted with similar skill. The large confidence intervals in Figure 3.8 and Table 3.1 and Table 3. 2, highlight the temporal sampling uncertainty associated with the small sample size of only 30 seasons.

Figure 3.9 shows the ROC and reliability (REL) diagrams of the forecast issued in November for above-normal conditions for the frequency of 5-day dry spells and frequency of days with THI higher than 78. These also confirm the above mentioned differences in skill and the uncertainties due to the temporal sampling. The ROC diagrams are above the one-on-one line for below and above normal conditions for both indicators, while they are close to the one-on-one line for normal conditions. The REL diagrams show a remarkable match with the one-on-one line for below- and above-normal conditions, while the REL diagram for normal conditions does not follow the one-on-one line. This shows that for above normal and below normal conditions, the frequency distribution of the forecast events is close to the distribution of verified forecast events (REL-diagram), and that the forecasts are skillful (ROC diagram).

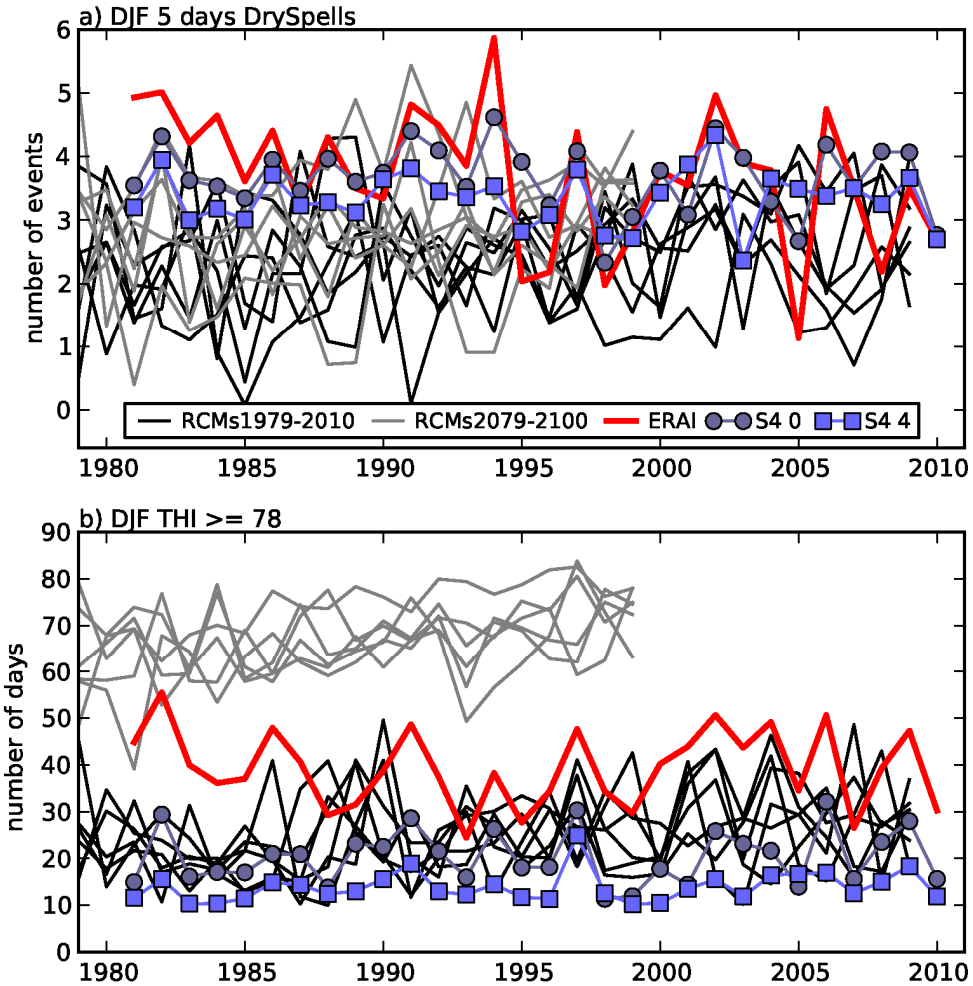

Figure 3.7. Time series of the DJF frequency of occurrence of 5 days dry spells (a) and frequency of occurrence of days with THI higher than 78 (b) averaged over the Limpopo region (see basin outline in previous maps). The time series are displayed for ERA-Interim (red line) and ECMWF S4 forecasts initialized in December (0 months lead time - dark blue) and August (4 months lead time - light blue). The black lines display the temporal evolution of the regional climate models between 1979 and 2010 and the gray lines between 2079 and 2100.

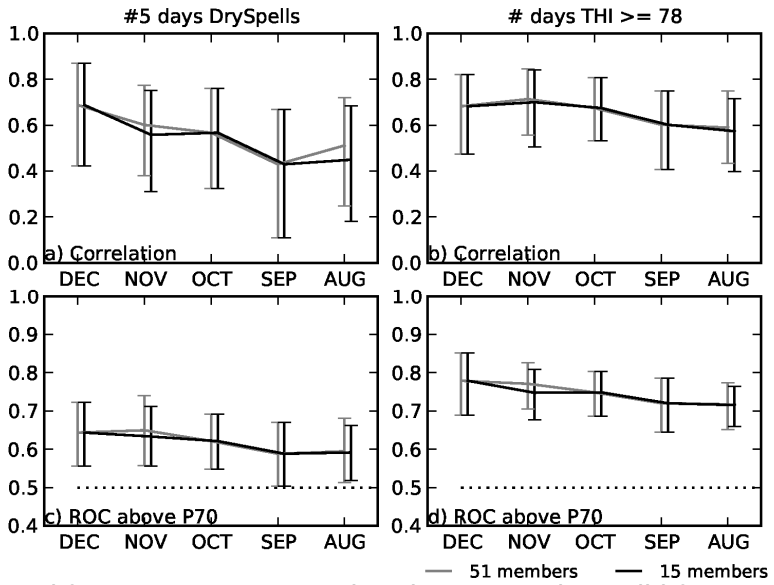

Figure 3.8. Seasonal forecast scores over the Limpopo region valid for DJF, at different lead times, for the frequency of occurrence of 5 days dry spells (a, c) and frequency of occurrence of days with THI higher than 78 (b, d). Mean grid-point correlation (a, b) and ROC of the forecast anomalies above the upper tercile (c, d). The error bars denote 95% confidence intervals estimated from 1000 bootstrap samples. The dark lines show the scores using the 15 ensemble members. The gray lines show the scores when using the full 51 ensemble members in the hindcast period (only available for the November and August initial forecast dates, for the other forecasts, the gray lines show the same as the dark lines).

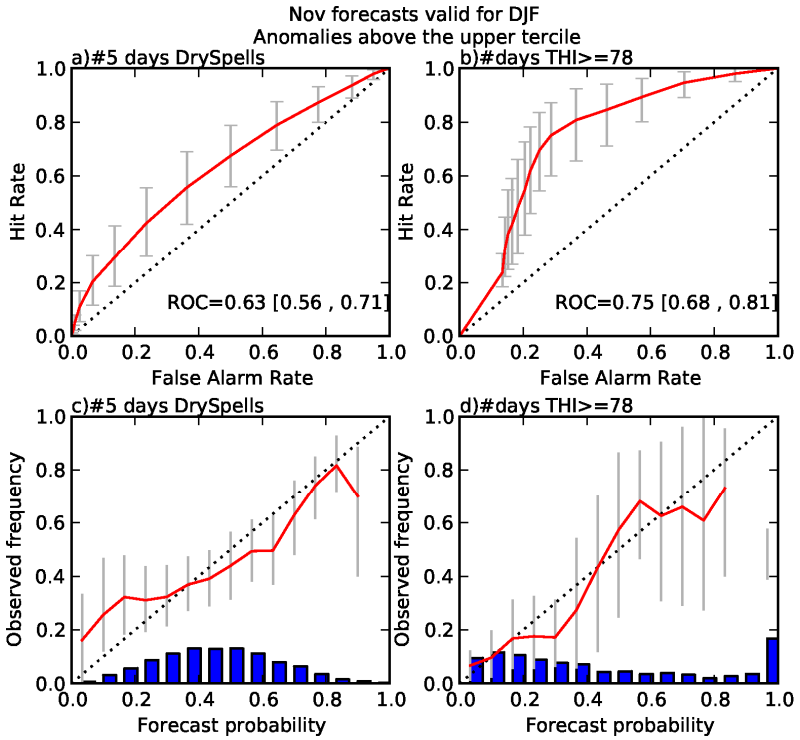

Figure 3.9. ROC (a,b) and REL (c,d) diagrams for the forecast anomalies above the upper tercile issued in November and valid for DJF over the Limpopo region: frequency of occurrence of 5 days dry spells (a, c) and frequency of occurrence of days with THI higher than 78 (b, d). The gray error bars denote 95% confidence intervals estimated from 1000 bootstrap samples.

3.4 Discussion

3.4.1 Implication of results

Forecast skill was represented in the context of climate change to demonstrate if seasonal forecasts may become more important in the future. In this discussion, we treat the two indicators (dry spell frequency and heat stress frequency) in order.

The climate change analysis showed that the heat stress days (THI above 72 for moderate stress and above 78 for severe stress) are projected to become much more frequent in the future. These results are confirmed by for example Nesamvuni et al. (2012), who also show that very severe stress conditions may occur in the distant future over Southern Africa. They express the heat stress conditions as mean annual values, while in this research increases in the frequency of occurrence of heat stress days are demonstrated. This indicates that if dairy (and other livestock) farming is to be continued on a large scale across Southern Africa, forecasting of these heat stress days becomes essential and represents one possible adaptation measure to climate change. Fortunately, the skill of predicting such heat stress conditions in current climate by seasonal forecasts has been demonstrated to be satisfactory for supporting decision-making. In particular skill for predicting below-normal and above-normal conditions is good, while skill of predicting normal conditions is low. The fact that heat stress conditions are increasing in frequency in the future and that seasonal forecasts can detect the frequency of occurrence of heat stress conditions skilfully, implies that seasonal forecasts will gain importance for the livestock sector. It should be noted that the best information on heat stress thresholds for livestock (THI higher than 72 and 78 respectively) is provided for cattle. Thresholds for small live stock are subject to future research.

For the frequency of dry spells, although their predictability is significant, the increase in importance of forecasts is limited, because their frequency of occurrence does not show increase from the RCM runs used in this study. Moreover, this study demonstrates that the skill of the predictions of dry spell frequency is much lower than the skill of predictions of frequency of heat stress days.

In general the results show that seasonal forecasts, translated into frequency of occurrence of indicators for critical weather conditions for the agricultural sector are skilful across Southern Africa. In particular, the predictability of the frequency of occurrence of heat stress days, expressed in the THI shows good predictability across all lead times considered. The predictability is pre-dominant for below-normal and above-normal conditions. For normal conditions, the skill is much lower. The analysis presented here discerns itself from other studies, by focusing on agricultural indicators, i.e. the frequency of dry spells and THI above thresholds, as meaningful indicators for subsistence farming. We acknowledge that these findings are also relevant to emerging farming, as well as the large-scale commercial farming sectors. A second distinguishing feature of the research is the focus on predicting intra-seasonal variability at seasonal time-scales, whilst previous studies for the southern African region have focused on the prediction of rainfall totals and average temperatures.

3.4.2 Forecast, warning and response chain

The results of this study show that forecasts of heat stress indicators are skilful, but will also become more important for end users such as farmers or institutions that support farmers in response measures, because their frequency of occurrence will increase in the future. Although these results are promising, it should be kept in mind that forecasting is merely one component of the forecasting, warning and response chain (see e.g. Carsell et al., 2004). If no proper mechanisms for warning are in place, if dissemination does not reach end users in an accessible or appropriate format (Archer, 2003), or no satisfactory mitigation actions or support for such actions are available to the end user, the forecast will still not lead to better preparedness. Furthermore, the real value of the forecast will depend on the amount of misses and false alarms, with respect to the amount of hits, combined with the costs of a wrong forecast, and the benefits of a correct forecast (Verkade and Werner, 2011). To assess

the real value, further insight into costs and benefits of possible decision supported by the forecasts would be needed.

3.4.3 Limitations of methods

The results of this study are subject to a number of assumptions and choices which are discussed in the following subsections.

Chosen emission scenario

First of all, the RCM projections analysed are all based on SRES A2 emission scenario. A2 is a high-end emission scenario, which implies drastic increases in surface temperature over southern Africa towards the end of the century. The resulting impacts on critical weather conditions may therefore turn out lower, if other emission scenarios with lower greenhouse gas concentrations are assumed. Further simulations could be done on less extreme emission scenarios and in particular on RCM simulations based on the more recent Representative Concentration Pathways (Van Vuuren et al., 2011).

Validity of absolute forecast numbers

It may be noted that the analysis performed here uses a 0.5 degree (~50 km) grid box scale. Across one grid box, variability in local climate conditions may occur due to e.g. differences in elevation, vegetation or other climate influencing factors. To translate the results to local conditions, further downscaling, either statistically or dynamically, is required. Insights to be gained from further downscaling are not likely to change the overall conclusions of this paper on climate change because such local variability will not impact significantly on the relative change of an indicator in time. However, in orographically highly variable areas, the absolute differences in temperature and rainfall conditions across space may vary significantly. This means that the seasonal forecasts may not fully represent the conditions of local farmers (i.e. at point scale) and are therefore in their current form not ready for use by such farmers. The absence of bias correction in the forecasts also impacts on the absolute accuracy of the forecast. If, however, regional results are to be used for decision-making and anomalies provide enough information to make or change a decision, then the results presented here could already be used. At a local scale, the use of medium-to-monthly range probabilistic forecasts might be more useful for day-to-day managing of the resources, as these suffer much less from model drift. The use of medium-to-monthly range forecasts remains, however, outside the scope of this paper.

Ground-truth

The skill analysis has been performed with a reanalysis dataset, rather than ground-truth observations. It is likely that the THI values, computed from the reanalysis are quite close to ground-truth, as the reanalysis data for temperature and dew point temperature are based on data assimilation of ground observations of these variables. Rainfall however, remains a modelled flux and is therefore much stronger conditioned by the ability of the ECMWF model to reproduce rainfall. Therefore, care should be taken that the comparison of the ERA-Interim and forecast climatology of the dry spell frequencies is a model-model comparison, while the THI frequencies are a model-data comparison.

Changes in seasonal forecast skill due to climate change

We have assumed that the skill of the S4 forecast system does not depend on the climate itself. It could be that the changes in climate in fact also change the predictability properties of the forecasts. For instance, changes in the El Niño Southern Oscillation (ENSO) may also alter the skill in areas where the climate is dominated by ENSO, or the teleconnections may become stronger or weaker. Nevertheless, the authors are of the opinion that possible changes in the predictability will not change the conclusions of this research.

3.5 Conclusions

Potential increases in the importance of seasonal forecasts for smallholder farming over Southern Africa and in particular the Limpopo basin in a changing climate have been investigated. This has been demonstrated a) by investigating whether the frequency of occurrence of critical weather conditions for the agricultural sector, in particular rain-fed farming and dairy farming, increases in the future according to RCM simulations, and b) by investigating the skill of seasonal forecasts to detect below normal, normal or above normal frequency of occurrence of these critical weather conditions in the December-January-February (DJF) season. The focus of critical weather conditions were the DJF frequency of occurrence of dry spells above 3 and 5 days (critical for rain-fed agriculture), as well as the DJF frequency of occurrence of Temperature Heat Index values above 72 and 78 (critical for cattle heat stress). If the frequency of occurrence of these indicator-threshold combinations is likely to increase significantly in comparison with current climate; and indicator-threshold combinations can be forecast with skill, it is likely that seasonal forecasts gain importance in the future, as they can lead more often to timely decision-making to mitigate the effect of a critical weather condition to the agricultural sector.

From the investigation it may be concluded that the seasonal forecasting of dry spells contains skill in particular for forecasts of 1 and 2 months lead time (and therefore already have potential value to end-users). However, they will not gain importance in the future, because the climate change projections used in this study do not show significant increase in their frequency of occurrence. The frequency of heat stress conditions however, is shown to drastically increase with great certainty in the future and can also be skilfully detected by seasonal forecasts within the DJF season (for all lead times, 1 to 4 months). Both types of indicators show a better skill in predicting above-normal and below-normal conditions than normal conditions. The frequency of heat stress conditions shows more skilful predictions than the skill of predicting frequency of dry spells. Concluding, it may be state that in particular the predictions of heat stress conditions already have potential value and will gain importance in the future. In interpreting these results, care should be taken that this study only made limited use of ground observations and that model drift in the seasonal forecasts causes inappropriate absolute values. As a result, only forecasts of anomalies were considered in this study. The climate change projections were based on the SRES A2 scenario, which is a high-end climate scenario. More conservative scenarios may result in less severe increases in heat stress conditions. Although this paper demonstrates skill in predicting critical weather conditions over Southern Africa, it is important to note that forecasts alone are not sufficient to alleviate their effects. Sufficient support for mitigation must be in place, and forecasts must be communicated in a context-specific, accessible and understandable format.

Table 3.1. ROC scores over the Limpopo of the forecasts anomalies of 3 and 5 days dry spells above the upper tercile, between the lower and upper terciles (normal) and below the lower tercile during DJF for different initial forecast dates (columns). The values between brackets are estimates of the +/- 95% confidence interval from 1000 bootstrap samples. The bootstrapping does not provide exactly symmetric confidence interval around the mean (but they are close to symmetric), but here the average is shown to reduce the amount of data in the table.

	Dec	Nov	Oct	Sep	Aug
Number of 3 days dry spells					
Above	0.61(0.06)	0.55(0.07)	0.58(0.07)	0.56(0.07)	0.57(0.06)
Normal	0.52(0.04)	0.50(0.03)	0.48(0.03)	0.52(0.03)	0.50(0.02)
Below	0.62(0.06)	0.56(0.07)	0.58(0.08)	0.56(0.07)	0.58(0.07)
Number of 5 days dry spells					
Above	0.64(0.08)	0.63(0.08)	0.62(0.07)	0.59(0.08)	0.59(0.07)
Normal	0.56(0.04)	0.47(0.03)	0.52(0.03)	0.53(0.03)	0.54(0.03)
Below	0.66(0.09)	0.63(0.08)	0.63(0.07)	0.60(0.08)	0.62(0.08)

Table 3. 2. As Table 3.1 *but for the number of days with THI >= 72 and THI >=78.*

	Dec	Nov	Oct	Sep	Aug
Number of days with THI >=72					
Above	0.69(0.08)	0.66(0.08)	0.64(0.07)	0.63(0.10)	0.58(0.09)
Normal	0.56(0.07)	0.56(0.06)	0.52(0.05)	0.49(0.05)	0.53(0.04)
Below	0.71(0.07)	0.63(0.10)	0.57(0.08)	0.61(0.10)	0.61(0.10)
Number of days with THI >=78					
Above	0.78(0.08)	0.75(0.07)	0.75(0.06)	0.72(0.07)	0.72(0.05)
Normal	0.61(0.07)	0.56(0.07)	0.57(0.05)	0.53(0.06)	0.56(0.05)
Below	0.76(0.08)	0.73(0.08)	0.69(0.07)	0.67(0.08)	0.69(0.06)

4. CONCLUSIONS

In this component of the DEWFORA research the impact of enhanced anthropogenic forcing on the attributes of drought over the African continent was explored. The analysis presented is largely based on high-resolution projections of climate change over Africa, performed as part of DEWFORA, and were obtained using a variable-resolution global model to downscale the projections of a number of CGCMs over Africa. The regional model simulations were first bias-corrected using observed monthly climatologies from CRU, before being used to study a number of drought metrics and their projected changes. The research conclusions also rely on the analysis of CGCM simulations of AR5 of the IPCC, and on the conclusions drawn from the CGCM projections described in AR4.

The Southern African region is projected to experience a general increase in the number of years with below-normal rainfall, although a decrease in dry years is also plausible over the central interior regions. The analysis of CGCM simulations reveal that an increase in extreme wet years over the regions is also plausible, that is, climate variability over the region is projected to increase. In the case of the Limpopo river basin (a DEWFORA case study area), the regional projections are particularly robust in indicating an increase in below-normal rainfall years. The Limpopo basin has been shown to be the part of the African continent that experiences the highest frequency of heat-waves under present-day climate, and drastic increases in heat-wave frequencies are projected for the basin, for both the mid- and far-futures. In fact, drastic increases in heat-wave frequencies are plausible over large parts of southern Africa by the end of the century. Most of the region is consistently projected to also experience an increase in the frequency of high fire danger days.

There is a consistent and robust message across the downscalings performed of East and tropical Africa experiencing a decrease in the number of years with below-normal rainfall. The CGCM simulations analysed confirm this result, also indicating an increase in the number of wet years for the region, and reduced rainfall variability. These results are also valid for the DEWFORA case study region of the Blue Nile river basin. Heat-waves do not occur over much of the tropics under present-day conditions, due to the tropics being prone to frequent convection. However, under future anthropogenic forcing, critical temperature thresholds over the region are being exceeded in response to general regional warming, resulting in an increasing frequency of occurrence of heat-waves over the region. The number of high fire danger days are consistently projected to increase over these regions.

More uncertainty surrounds the projected futures of the number of years with below-normal rainfall over West Africa, including the DEWFORA case study region of the Niger basin. A mixed signal, of both increases and decreases in the number of years with below-normal rainfall, is projected. However, further to north over North Africa and its Mediterranean coast, another robust signal exists in the projections. These regions are projected to see drastic increases in the number of years with below-normal rainfall, and a decrease in wet years. Signals of drying and more years of below-normal rainfall are also valid for the DEWFORA case study of the Oum-er-Rbia basin. These North African regions are also robustly projected to experience drastic increases in heat-wave frequencies during the 21st century.

Given the ample evidence of plausible increases in the frequency of occurrence of years of below-normal or above-normal rainfall over much of the continent, and the robust signal of heat-wave frequencies increasing over Africa under climate change, the skilful projection of these quantities at seasonal timescales may be expected to become more important. These aspects were explored in some detail over the Limpopo river basin, a case study region with a long history of quality atmospheric observations that allow for in depth model verification studies. It was shown that the state-of-the-art ECMWF seasonal forecasting system can skilfully predict the intra-seasonal variability of heat-waves and spells over the region, at seasonal time-scales. This is an encouraging result, indicating the potential of skilful seasonal forecasts as an adaptation mechanism to climate change.

5. REFERENCES

Archer, E. R. M.: Identifying Underserved End-User Groups in the Provision of Climate Information, Bull. Am. Meteorol. Soc., 84(11), 1525–1532, doi:10.1175/BAMS-84-11-1525, 2003.

Archer van Garderen, E. R. M.: (Re) Considering Cattle Farming in Southern Africa under a Changing Climate, Weather Clim. Soc., 3(4), 249–253, doi:10.1175/WCAS-D-11-00026.1, 2011. 1990.

Alexander, M.E.: Computer calculation of the Keetch-Byram Drought Index – programmers beware! Fire Management Notes, 51, 23-25, 1990.

Barnston, A. G. and Smith, T. M.: Specification and Prediction of Global Surface Temperature and Precipitation from Global SST Using CCA, J. Clim., 9(11), 2660–2697, doi:10.1175/1520-0442(1996)009<2660:SAPOGS>2.0.CO;2, 1996.

Barron, J. and Okwach, G.: Run-off water harvesting for dry spell mitigation in maize (Zea mays L.): results from on-farm research in semi-arid Kenya, Agric. Water Manag., 74(1), 1–21, doi:10.1016/j.agwat.2004.11.002, 2005.

Barron, J., Rockström, J., Gichuki, F. and Hatibu, N.: Dry spell analysis and maize yields for two semi-arid locations in east Africa, Agric. For. Meteorol., 117(1-2), 23–37, doi:16/S0168-1923(03)00037-6, 2003.

Belo-Pereira, M., Dutra, E. and Viterbo, P.: Evaluation of global precipitation datasets over the Iberian Peninsula, J Geophys Res, 116, D20101, doi:10.1029/2010jd015481, 2011.

Brown, C. and Hansen, J.: Agricultural water management and climate risk. Report to the Bill and Melinda Gates Foundation. IRI Tech. Rep. No. 08-01, International Research Institute for Climate mand Society, New York, USA., 2008.

Carsell, K. M., Pingel, N. D. and Ford, D. T.: Quantifying the Benefit of a Flood Warning System, Nat. Hazards Rev., 5(3), 131–140, doi:10.1061/(ASCE)1527-6988(2004)5:3(131), 2004.

Christensen et al.: Regional Climate Projections. In: Climate Change 2007: The Physical Science Basis. Contribution of Working Group I to the Fourth Assessment Report of the Intergovernmental Panel on Climate Change. Cambridge University Press, Cambridge, United Kingdom and New York, NY, USA, 2007.

Conway, D., Persechino, A., Ardoin-Bardin, S., Hamandawana, H., Dieulin, C., Mahé, G.: Rainfall and Water Resources Variability in Sub-Saharan Africa during the Twentieth Century. J. Hydrometeor, 10, 41–59, 2009.

Davis, C.: Climate Risk and Vulnerability: a handbook for southern Africa, Coucil for Scientific and Industrial Research, Pretoria, South Africa., n.d.

Dee, D. P., Uppala, S. M., Simmons, A. J., Berrisford, P., Poli, P., Kobayashi, S., Andrae, U., Balmaseda, M. A., Balsamo, G., Bauer, P., Bechtold, P., Beljaars, A. C. M., van de Berg, L., Bidlot, J., Bormann, N., Delsol, C., Dragani, R., Fuentes, M., Geer, A. J., Haimberger, L., Healy, S. B., Hersbach, H., Hólm, E. V., Isaksen, L., Kållberg, P., Köhler, M., Matricardi, M., McNally, A. P., Monge-Sanz, B. M., Morcrette, J. ., Park, B. K., Peubey, C., de Rosnay, P., Tavolato, C., Thépaut, J. N. and Vitart, F.: The ERA-Interim reanalysis: configuration and performance of the data assimilation system, Q. J. R. Meteorol. Soc., 137(656), 553–597, doi:10.1002/qj.828, 2011.

Dikmen, S. and Hansen, P. J.: Is the temperature-humidity index the best indicator of heat stress in lactating dairy cows in a subtropical environment?, J. Dairy Sci., 92(1), 109–116, doi:10.3168/jds.2008-1370, 2009.

Dowdy, A.J., Mills, G.A., Finkele, K. and De Groot, W.: Index sensitivity analysis applied to the Canadian Forest Fire Weather Index and the McArthur Forest Fire Danger Index. Meteorological Applications 17, 298-312, 2010.

Dutra, E., Di Giuseppe, F., Wetterhall, F. and Pappenberger, F.: Seasonal forecasts of droughts in African basins using the Standardized Precipitation Index, Hydrol Earth Syst Sci, 17(6), 2359–2373, doi:10.5194/hess-17-2359-2013, 2013.

Engelbrecht, F.A. and Bopape, M.J.: High-resolution projected climate futures for southern Africa. 27th Annual Conference of the South African Society for Atmospheric Sciences, September 2011, Hartebeeshoek. ISBN 978-0-620-47333-0, 2011.

Engelbrecht, C. J., Engelbrecht, F. A. and Dyson, L. L.: High-resolution model-projected changes in mid-tropospheric closed-lows and extreme rainfall events over southern Africa, Int. J. Clim., 33(1), 173–187, doi:10.1002/joc.3420, 2013.

Engelbrecht, F. A., Landman, W. A., Engelbrecht, C. J., Landman, S., Bopape, M. M., Roux, B., McGregor, J. L. and Thatcher, M.: Multi-scale climate modelling over Southern Africa using a variable-resolution global model, Water SA, 37(5), 647–658, 2011.

Engelbrecht, F. A., McGregor, J. L. and Engelbrecht, C. J.: Dynamics of the Conformal-Cubic Atmospheric Model projected climate-change signal over southern Africa, Int. J. Clim., 29(7), 1013–1033, doi:10.1002/joc.1742, 2009.

Engelbrecht, F.A., Naidoo, M., Bopape, M.J.: Meteorological climate scenarios for Africa and specific case study regions of the Nile and Niger River basins, DEWFORA D3.4, 2013.

Fournet,S., Eldin,A., Engelbrecht,F., Aich,V., Amin,D., Fouda, S., Hattermann,F., Huang, S., Kassem, T.,Hagen, K, Krysanova,V., Liersch,S., Mahdy, A., Tecklenburg, J. and Vetter, T.: Hydrological climate scenarios for Africa and specific case study regions of the Nile and Niger river basins, DEWFORA D3.5, 2013.

Gerrits, A. M. J., Savenije, H. H. G., Hoffmann, L. and Pfister, L.: New technique to measure forest floor interception – an application in a beech forest in Luxembourg, Hydrol Earth Syst Sci, 11(2), 695–701, 2007.

De Groen, M. M. and Savenije, H. H. G.: A monthly interception equation based on the statistical characteristics of daily rainfall, Water Resour. Res., 42, 10 PP., doi:200610.1029/2006WR005013, 2006.

Hetem, R. S., de Witt, B. A., Fick, L. G., Fuller, A., Maloney, S. K., Meyer, L. C. R., Mitchell, D. and Kerley, G. I. H.: Effects of desertification on the body temperature, activity and water turnover of Angora goats, J. Arid Environ., 75(1), 20–28, doi:10.1016/j.jaridenv.2010.08.007, 2011.

Holtslag, A. A. M., Boville, B.A.: Local Versus Nonlocal Boundary-Layer Diffusion in a Global Climate Model, J. Climate, 6, 1825–1842, 1993.

Hulme, M., Doherty, R. and Ngara, T.: African climate change: 1900-2100, Clim. Res. 17, 145-168, 2001.

Husak, G. J., Michaelsen, J. and Funk, C.: Use of the gamma distribution to represent monthly rainfall in Africa for drought monitoring applications, International Journal of Climatology, 27: 935–944. doi: 10.1002/joc.1441, 2007.

Ingram, K. ., Roncoli, M. . and Kirshen, P. .: Opportunities and constraints for farmers of west Africa to use seasonal precipitation forecasts with Burkina Faso as a case study, Agric. Syst., 74(3), 331–349, doi:10.1016/S0308-521X(02)00044-6, 2002.
Kane, R. P.: Periodicities, ENSO effects and trends of some South African rainfall series: an update, South Afr. J. Sci., 105(5-6), 199–207, 2009.

Katzfey, J.J., McGregor, J.L., Nguyen, K.C., Thatcher, M.: Dynamical downscaling techniques: Impacts on regional climate change signals. In: Anderssen RS, Braddock RD and Newham LTH (eds.). MODSIM09 Int. Congress on Modelling and Simulation. URL: www.mssanz.org.au/modsim09/I13/katzfey_I13.pdf 2377-2383, 2009.

Keetch, J.J. and Byram, G.M.: A drought index for fire control. Res. Pap. SE-38. Asheville NC: U.S. Department of Agriculture, Forest Service, Southeastern Forest Experiment Station. 32 p (Revised November 1988).

Kowalczyk, E. A., Wang, Law, R.M., Davies, H.L., McGregor, J.L. and Abramowitz, G.: The CSIRO Atmosphere Biosphere Land Exchange (CABLE) model for use in climate models and as an offline model. CSIRO Marine and Atmospheric Research Paper 13, 37 pp, 2006.

Kusangaya, S., Warburton, M. L., Archer Van Garderen, E. R. M. and Jewitt, G. P.: Impacts of Climate Change on Water Resources in Southern Africa: A Review, Phys Chem Earth, in revision.

Lal, M., McGregor, J. L. and Nguyen, K. C.: Very high-resolution climate simulation over Fiji using a global variable-resolution model, Clim. Dyn., 30(2-3), 293–305, doi:10.1007/s00382-007-0287-0, 2008.

Landman, W.A. and Beraki, A.: Multi-model forecast skill for mid-summer rainfall over southern Africa, International Journal of Climatology, vol. 32(2), pp 303-314, 2012.

Landman, W.A., DeWitt, D., Lee, D.-E., Beraki, A. and Lötter, D.: Seasonal Rainfall Prediction Skill over South Africa: One- versus Two-Tiered Forecasting Systems, Wea. Forecasting, 27, 489–501. doi: http://dx.doi.org/10.1175/WAF-D-11-00078.1, 2012.

Landman, W. A., Engelbrecht, F. A., Beraki, A., Engelbrecht, C., Mbedzi, M., Gill, T. and Ntsangwane, L.: Model output statistics applied to multi-model ensemble long-range forecasts over South Africa, Project Report, Water Research Commission, Pretoria, South Africa., 2009.

Laraque, A., Mahé, G., Orande, D., Marieu, B. : Spatiotemporal variations in hydrological regimes within Central Africa during the XXth century, Journal of Hydrology, 245, 104–107, 2001.

LIMCOM: Joint Limpopo River Basin Study Scoping Phase: Final Report, Republica de Mocambique, Ministerio Das Obras Publicas e Habitacao - Direccao Nacional De Aguas/Limpopo Basin Permanent Technical Committee, Mozambique., 2010.

Lloyd-Hughes, B. and Saunders, M.A.: A drought climatology for Europe, Int. J. Climatol., 22, 1571–1592, 2002.

Love, D., Uhlenbrook, S., Twomlow, S. and Van der Zaag, P.: Changing hydroclimatic and discharge patterns in the northern Limpopo basin, Zimbabwe, Water SA Online, 36(3), 335–350, 2010.

Lu, J., Vecchi, G. A., & Reichler, T. (2007). Expansion of the Hadley cell under global warming. Geophysical Research Letters, 34(6).

Malherbe, J., Engelbrecht, F. A. and Landman, W. A.: Projected changes in tropical cyclone climatology and landfall in the Southwest Indian Ocean region under enhanced anthropogenic forcing, Clim. Dyn., 40(11-12), 2867–2886, doi:10.1007/s00382-012-1635-2, 2013.

McGregor, J.L.: Semi-Lagrangian advection on conformal-cubic grids, Mon. Wea. Rev., 124, 1311-1322, 1996.

McGregor, J.L.: A new convection scheme using a simple closure. In "Current issues in the parameterization of convection", BMRC Research Report 93, 33-36, 2003.

McGregor, J. L.: C-CAM geometric aspects and dynamical formulation, in CSIRO Atmospheric Research Technical paper, vol. 70, CSIRO Atmospheric Research, Aspendale, Vic., Australia., 2005b.

McGregor, J.L.: Geostrophic adjustment for reversibly staggered grids, Mon. Wea. Rev., 133, 1119-1128, 2005a.

McGregor, J.L. and Dix, M.R.: The CSIRO conformal-cubic atmospheric GCM. In IUTAM Symposium on Advances in Mathematical Modelling of Atmosphere and Ocean Dynamics, P. F. Hodnett (Ed.), Kluwer, Dordrecht, 197-202, 2001.

McGregor, J. L. and Dix, M. R.: An Updated Description of the Conformal-Cubic Atmospheric Model, in High Resolution Numerical Modelling of the Atmosphere and Ocean, edited by K. Hamilton and W. Ohfuchi, pp. 51–75, Springer New York. [online] Available from: http://link.springer.com/chapter/10.1007/978-0-387-49791-4_4 (Accessed 31 July 2013), 2008.

McGregor, J.L., Katzfey, J.J., Nguyen, K.C. and Thatcher, M.J.: Some recent developments for dynamic downscaling of climate. Proc. 27th Annual Conference of the South African Society for Atmospheric Sciences. September 2011, Hartebeesboek, 2011.

McKee, T.B., Doesken, N.J., Kleist, J.: The Relationship of Drought Frequency and Duration to Time Scales. Proc. 8th Conf. on Appl. Clim., 17-22 Jan. 1993, Anaheim, CA, 179-184, 1993.

McKee, T. B., Doesken, N.J. and Kleist, J.: Drought monitoring with multiple time scales. Proc. Ninth Conf. on Applied Climatology, Dallas, TX, Amer. Meteor. Soc. 233-236, 1995.

Meadows, M.E.: Global change and southern Africa. Geographical Research **44**, 135-145, 2006.

Mitchell, T. D. and Jones, P. D.: An improved method of constructing a database of monthly climate observations and associated high-resolution grids, Int. J. Clim., 25(6), 693–712, doi:10.1002/joc.1181, 2005.

Molteni, F., Stockdale, T., Balsameda, M., Balsamo, G., Buizza, R., Ferranti, L., Magnusson, L., Mogensen, K., Palmer, T. and Vitart, F.: The new ECMWF seasonal forecast system (System 4), ECMWF Tech. Memo 656, ECMWF, Reading, U.K., 2011.
Mwangi, E., Wetterhall, F., Dutra, E., Di Giuseppe, F. and Pappenberger, F.: Forecasting Droughts in East Africa (submitted), Hydr Earth Syst Sci Discuss, submitted.

Nardone, A., Ronchi, B., Lacetera, N., Ranieri, M. S. and Bernabucci, U.: Effects of climate changes on animal production and sustainability of livestock systems, Livest. Sci., 130(1–3), 57–69, doi:10.1016/j.livsci.2010.02.011, 2010.

Nesamvuni, E., Lekalakala, R., Norris, D. and Ngambi, J. W.: Eff. Clim. Change Dairy Cattle South Afr., 7(26), 3867–3872, 2012.

Nicholson, S.E.: Climatic and environmental change in Africa during the last two centuries. Climate Research, 17, 123-144, 2001.

Nunez, M. and McGregor, J. L.: Modelling future water environments of Tasmania, Australia, Clim. Res., 34(1), 25–37, doi:10.3354/cr034025, 2007.

Nyakudya, I. W. and Stroosnijder, L.: Water management options based on rainfall analysis for rainfed maize (Zea mays L.) production in Rushinga district, Zimbabwe, Agric. Water Manag., 98(10), 1649–1659, doi:10.1016/j.agwat.2011.06.002, 2011.
O'brien, S. P.: Anticipating the Good, the Bad, and the Ugly An Early Warning Approach to Conflict and Instability Analysis, J. Confl. Resolut., 46(6), 791–811, doi:10.1177/002200202237929, 2002.

Ochola, W. O. and Kerkides, P.: A Markov chain simulation model for predicting critical wet and dry spells in Kenya: analysing rainfall events in the Kano Plains, Irrig. Drain., 52(4), 327–342, doi:10.1002/ird.94, 2003.

Olwoch, J.M., Reyers, B., Engelbrecht, F.A. and Erasmus, B.F.N.: Climate change and the tick-borne disease, Theileriosis (East Coast fever) in sub-Saharan Africa, Journal of Arid Environments **72**, 108-120, 2008.

Orlowsky, B. and Seneviratne, S. I.: Global changes in extreme events: Regional and seasonal dimension, Climatic Change, 110, 669–696, 2012.

Orlowsky, B., & Seneviratne, S. I.: Elusive drought: uncertainty in observed trends and short- and long-term CMIP5 projections. Hydrology and Earth System Sciences, 17(5), 1765-1781, 2013.

Parr, J. F., Stewart, B. A., Hornick, S. B. and Singh, R. P.: Improving the Sustainability of Dryland Farming Systems: A Global Perspective, in Advances in Soil Science, edited by R. P. Singh, J. F. Parr, and B. A. Stewart, pp. 1–8, Springer New York. [online] Available from: http://link.springer.com/chapter/10.1007/978-1-4613-8982-8_1 (Accessed 17 July 2013), 1990.

Ramos, M. H., van Andel, S. J. and Pappenberger, F.: Do probabilistic forecasts lead to better decisions?, Hydrol Earth Syst Sci, 17(6), 2219–2232, doi:10.5194/hess-17-2219-2013, 2013.

Ramos, M.-H., Mathevet, T., Thielen, J. and Pappenberger, F.: Communicating uncertainty in hydro-meteorological forecasts: mission impossible?, Meteorol. Appl., 17(2), 223–235, doi:10.1002/met.202, 2010.

Ravagnolo, O., Misztal, I. and Hoogenboom, G.: Genetic Component of Heat Stress in Dairy Cattle, Development of Heat Index Function, J. Dairy Sci., 83(9), 2120–2125, doi:10.3168/jds.S0022-0302(00)75094-6, 2000.

Reason, C. J. C., Hachigonta, S. and Phaladi, R. F.: Interannual variability in rainy season characteristics over the Limpopo region of southern Africa, Int. J. Clim., 25(14), 1835–1853, doi:10.1002/joc.1228, 2005.

Rockström, J.: Water resources management in smallholder farms in Eastern and Southern Africa: An overview, Phys. Chem. Earth Part B Hydrol. Oceans Atmosphere, 25(3), 275–283, doi:10.1016/S1464-1909(00)00015-0, 2000.

Rockström, J.: Water for food and nature in drought–prone tropics: vapour shift in rain–fed agriculture, Philos. Trans. R. Soc. Lond. B. Biol. Sci., 358(1440), 1997–2009, doi:10.1098/rstb.2003.1400, 2003.

Rotstayn, L.D.: A physically based scheme for the treatment of stratiform clouds and precipitation in large-scale models. I: Description and evaluation of the microphysical processes. Quart. J. Roy. Meteor. Soc., 123 1227-1282, 1997.

Ruosteenoja, K., Carter T.R., Jylha, K. Tuomenvirta, H.: Future Climate in World Regions: An Intercomparison of Model-Based Projections for the New IPCC Emissions Scenarios. Finnish Environment Institute, Helsinki, 83 pp, 2003.

Russo, S., Barbosa, P., Dosio, A., Sterl, A., & Vogt, J.: Projection of occurrence of extreme dry-wet years and seasons in Europe with stationary and non-stationary Standardized Precipitation Index. In EGU General Assembly Conference Abstracts (Vol. 15, p. 3877), 2013.

RVAC: SADC Regional Vulnerability Assessment and Analysis (RVAA) Synthesis Report: State of Food Insecurity and Vulnerability in the Southern Africa Development Community, RVAA Annual Dissemination Forum, Johannesburg, South Africa., 2011.

Savenije, H. H. G.: The importance of interception and why we should delete the term evapotranspiration from our vocabulary, Hydrol Process, 18, 1507–1511, 2004.
Usman, M. T. and Reason, C. J. C.: Dry spell frequencies and their variability over southern Africa, Clim. Res., 26(3), 199–211, doi:10.3354/cr026199, 2004.

Seidel, D. J., Fu, Q., RanDel, W. J., & ReichleR, T. J.: Widening of the tropical belt in a changing climate. Nature Geoscience, 1(1), 21-24, 2007.

Sheffield, J. and Wood, E.: Projected changes in drought occurrence under future global warming from multi-model, multiscenario, IPCC AR4 simulations, Clim. Dynam., 31, 79–105, 2008.

Thatcher, M. and McGregor, J.L.: Using a scale-selective filter for dynamical downscaling with the conformal cubic atmospheric model, Monthly Weather Review **137**, 1742-1752, 2009.

Thatcher, M. and McGregor, J.L.: A technique for dynamically downscaling daily-averaged GCM datasets over Australia using the Conformal Cubic Atmospheric Model, Monthly Weather Review, 139, 79-95, 2010.

Thom, H.C.: A note on the gamma distribution. Monthly Weather Review 86: 117–122, 1958.

Thornton, P.K., Jones, P.G., Ericksen, P.J., Challinor, A.J.: Agriculture and food systems in sub-Saharan Africa in a 4 C+ world. Phil. Trans. R. Soc. **369**, 117-136. DOI: 10.1098/rsta.2010.0246, 2011.

Seidel DJ. Fu Q. Randel WJ. Reichler TJ. 2008. Widening of the tropical belt in a changing climate. Nature Geoscience **1**, 21-24.

Van Wilgen, B.W., Forsyth, G.G., De Klerk, H., Das, S., Khuluse, S. and Schmitz, P.: Fire management in Mediterranean-climate shrublands: a case study from the Cape fynbos, South Africa, Journal of Applied Ecology 47 631–638 DOI: 10.1111/j.1365-2664.2010.01800, 2010.

Verkade, J. S. and Werner, M. G. F.: Estimating the benefits of single value and probability forecasting for flood warning, Hydrol Earth Syst Sci, 15(12), 3751–3765, doi:10.5194/hess-15-3751-2011, 2011.

Van Vuuren, D. P., Edmonds, J., Kainuma, M., Riahi, K., Thomson, A., Hibbard, K., Hurtt, G. C., Kram, T., Krey, V., Lamarque, J.-F., Masui, T., Meinshausen, M., Nakicenovic, N., Smith, S. J. and Rose, S. K.: The representative concentration pathways: an overview, Clim. Change, 109(1-2), 5–31, doi:10.1007/s10584-011-0148-z, 2011.

Voldoire, A., E. Sanchez-Gomez, D. Salas y Mélia, B. Decharme, C. Cassou, S.Sénési, S. Valcke, I. Beau, A. Alias, M. Chevallier, M. Déqué, J. Deshayes, H. Douville, E. Fernandez, G. Madec, E. Maisonnave , M.-P. Moine, S. Planton, D.Saint-Martin, S. Szopa, S. Tyteca, R. Alkama, S. Belamari, A. Braun, L. Coquart, F. Chauvin: The CNRM-CM5.1 global climate model: description and basic evaluation, Clim. Dyn., accepted, DOI:10.1007/s00382-011-1259-y, 2011.

Wilks D.S.: Statistical Methods in the Atmospheric Sciences. Elsevier Academic Press Publications: pp. 467, 2002.

Ziervogel, G., Archer van Garderen, E., Midgley, G., Hamann, R., Taylor, A., Stuart-Hill, S., Warburton-Toucher, M. and Myers, J.: Climate change impacts and adaptation in South Africa: current approaches and future challenges, WiRES Clim. Change, in revision.